

Lithology of Evaporite Cycles and
Cycle Boundaries in the Upper Part of the
Paradox Formation of the Hermosa Group of
Pennsylvanian Age in the Paradox Basin,
Utah and Colorado

U.S. GEOLOGICAL SURVEY BULLETIN 2000-B



On the Front Cover: View south toward LaSal Mountains along Colorado River between Cisco and Moab, Utah. Fisher Towers in center are composed of Permian Cutler Formation and capped by Triassic Moenkopi Formation. Prominent mesa at left center is capped by Jurassic Kayenta Formation and Wingate Sandstone and underlain by slope-forming Triassic Chinle and Moenkopi Formations. The Chinle-Moenkopi contact is marked by a thin white ledge-forming gritstone. Valley between Fisher Towers and Fisher Mesa in background is part of Richardson Amphitheater part of Professor Valley. Photograph by Omer B. Raup, U.S. Geological Survey.

Lithology of Evaporite Cycles and Cycle Boundaries in the Upper Part of the Paradox Formation of the Hermosa Group of Pennsylvanian Age in the Paradox Basin, Utah and Colorado

By OMER B. RAUP *and* ROBERT J. HITE

EVOLUTION OF SEDIMENTARY BASINS—PARADOX BASIN
A.C. HUFFMAN, JR., Project Coordinator

U.S. GEOLOGICAL SURVEY BULLETIN 2000-B

*A multidisciplinary approach to research studies of sedimentary
rocks and their constituents and the evolution of
sedimentary basins, both ancient and modern*



UNITED STATES GOVERNMENT PRINTING OFFICE, WASHINGTON : 1992

U.S. DEPARTMENT OF THE INTERIOR
MANUEL LUJAN, JR., Secretary

U.S. GEOLOGICAL SURVEY
Dallas L. Peck, Director

For sale by the Books and Open-File Reports Section
U.S. Geological Survey
Federal Center, Box 25286
Denver, CO 80225

Any use of trade, product, or firm names in this publication is for descriptive purposes only and does not imply endorsement by the U.S. Government

Library of Congress Cataloging-in-Publication Data

Evolution of sedimentary basins—Paradox Basin.

p. cm. — (U.S. Geological Survey bulletin ; 2000)

Includes bibliographical references.

Contents: ch. B. Lithology of evaporite cycles and cycle boundaries in the upper part of the Paradox Formation of the Hermosa Group of Pennsylvanian age in the Paradox Basin, Utah and Colorado / by Omer B. Raup and Robert J. Hite.

Supt. of Docs. no.: I 19.3:2000 (v. 2)

1. Geology—Paradox Basin. I. Raup, Omer B. (Omer Beaver), 1930-. II. Hite, R. J. (Robert J.) III. Series.

QE75.B9 no. 2000, etc.

[QE79]

552'.5—dc20

92-15577
CIP

CONTENTS

Abstract.....	B1
Introduction.....	1
Geologic Setting	1
Core Description.....	3
Delhi-Taylor Oil Company Cane Creek No. 1	3
Delhi-Taylor Oil Company Shafer No. 1	4
Evaporite Cycles.....	5
Lithologic Characteristics of Cycles 2 and 3 of the Paradox Formation.....	6
Interbeds	6
Anhydrite (transgressive).....	6
Silty Dolomite (transgressive).....	13
Black Shale	14
Dolomite (regressive)	15
Anhydrite (regressive).....	16
Halite Beds.....	18
Anhydrite Laminations	21
Bromine Distribution	26
Potash Deposits.....	29
Interbed Contact Relationships.....	30
Detailed Correlation of Cycle 3 Interbeds Between Cane Creek No. 1 and Shafer No. 1	
Core Holes	31
Sea-Level Control During Evaporite Deposition	33
Summary of Evidence for Environments of Deposition of Evaporites in the Paradox	
Basin	35
References Cited.....	36

FIGURES

1. Map of Paradox Basin, southwestern Colorado and southeastern Utah, showing limits of evaporite facies in the Paradox Formation	B2
2-4. Schematic stratigraphic columns of:	
2. Cane Creek No. 1 core hole	4
3. Shafer No. 1 core hole	5
4. Cycle 2 facies in Cane Creek No. 1 core	6
5. Diagram showing correlation of lithologic units in Shafer No. 1 and Cane Creek No. 1 core	7
6. Charts showing mineral composition of penesaline and clastic intervals in Cane Creek No. 1 core as determined by X-ray diffraction.....	8
7-12. Photographs of polished surface of core:	
7. Cane Creek No. 1, depth 2,460.5 ft	10
8. Shafer No. 1, depth 2,588 ft.....	10
9. Cane Creek No. 1, depth 2,456.5 ft	11
10. Cane Creek No. 1, depth 2,455.3 ft	11
11. Shafer No. 1, depth 2,583.5 ft.....	12
12. Shafer No. 1, depth 2,581.5 ft.....	12
13. Photograph of segment of Cane Creek No. 1 core, depth 2,438 ft.....	14
14. Photograph of polished surface of core from Shafer No. 1 core, depth 2,569 ft.....	14
15. Photomicrograph of transgressive dolomite from Cane Creek No. 1 core, depth 2,433.5 ft	15
16. Photograph of polished surface of core from Shafer No. 1 core, depth 2,542 ft.....	15

17.	Photomicrograph of black shale from Cane Creek No. 1 core, depth 2,410.5 ft	16
18–24.	Photographs of polished surface of cores from:	
18.	Shafer No. 1, depth 2,523.5 ft.....	16
19.	Cane Creek No. 1, depth 2,372 ft	17
20.	Shafer No. 1, depth 2,517.5 ft.....	17
21.	Cane Creek No. 1, depth 2,366 ft	18
22.	Cane Creek No. 1, depth 2,364.2 ft	18
23.	Cane Creek No. 1, depth 2,356.7 ft	19
24.	Cane Creek No. 1, depth 2,353.7 ft	19
25.	Photographs of polished surface of core from Shafer No. 1 at consecutive depths, 2,500–2,505 ft.....	20
26–35.	Photographs of segment of:	
26.	Cane Creek No. 1 core, depth 2,336.5 ft	22
27.	Cane Creek No. 1 core, depth 2,265 ft	23
28.	Shafer No. 1 core, depth 2,860 ft.....	24
29.	Shafer No. 1 core, depth 3,673 ft.....	25
30.	Cane Creek No. 1 core, depth 2,623.5 ft	25
31.	Cane Creek No. 1 core, depth 2,616.5 ft	26
32.	Shafer No. 1 core, depth 2,610.5 ft.....	26
33.	Shafer No. 1 core, depth 2,491 ft.....	27
34.	Cane Creek No. 1 core, depth 2,340.4 ft	27
35.	Cane Creek No. 1 core, depth 2,218.5 ft	28
36–37.	Profiles of bromine distribution in halite bed of:	
36.	Cycle 2, Cane Creek No. 1 core	29
37.	Cycle 3, Cane Creek No. 1 core	30
38–40.	Photographs of polished surface of core from Shafer No. 1:	
38.	Depth 2,655 ft	31
39.	Depth 3,303 ft	31
40.	Depth 3,528.5 ft.....	32
41, 42.	Photographs of segment of:	
41.	Shafer No. 1 core, depth 3,892 ft.....	32
42.	Cane Creek No. 1 core, depth 2,640.5 ft	33
43–45.	Photographs of polished surface of core from Shafer No. 1:	
43.	Depth 2,869.5 ft.....	34
44.	Depth 3,919.5 ft.....	34
45.	Depth 4,149.5 ft.....	35

LITHOLOGY OF EVAPORITE CYCLES AND CYCLE BOUNDARIES IN THE UPPER PART OF THE PARADOX FORMATION OF THE HERMOSA GROUP OF PENNSYLVANIAN AGE IN THE PARADOX BASIN, UTAH AND COLORADO

By OMER B. RAUP *and* ROBERT J. HITE

ABSTRACT

Evaporites of the Paradox Formation of the Hermosa Group of Pennsylvanian age in the Paradox Basin of southeastern Utah and southwestern Colorado are direct precipitates from marine brines and have been changed only slightly by subsequent events. Geophysical logs of deep wells indicate that the Paradox Formation is composed of 29 halite-bearing evaporite cycles. Rock types that make up the cycles, in order of increasing salinity, are organic-carbon-rich carbonate shale (black shale), dolomite, anhydrite, and halite (with or without potash). Studies of core from two core holes in the central part of the basin show that some of the cycles in the upper part of the Paradox Formation are remarkably complete, indicating regular changes in salinity. Newly recognized lithologic textures and cycle boundaries in 11 evaporite cycles indicate very regular cyclicity of subaqueous sedimentation in a basin in which salinity was probably controlled by Gondwana glaciation.

INTRODUCTION

The Paradox Basin of southeastern Utah and southwestern Colorado contains a thick section of evaporites in the Paradox Formation of the Hermosa Group of Pennsylvanian age. This section contains 29 well-defined cycles composed of halite beds and associated penesaline and siliciclastic rocks (interbeds) (Hite, 1960).

Dissolution unconformities that separate each of the evaporite cycles in the Paradox Formation were recognized by Hite (1970). Since then, much detailed work has been done to characterize the sedimentological sequence within the cycles. The present study was done using cores from two core holes drilled during potash exploration in two areas southwest of Moab, Utah. These cores were taken from the

upper part of the Paradox Formation in cycles 2–11 and part of cycle 13. In this paper we describe some of the important features of these evaporite cycles that serve as the basis for interpretations of the mode of deposition of these rocks.

Acknowledgments.—We thank James Hodgkinson and David Hogle for preparing the polished core samples, Samuel J. Dennis, Robert H. Weir, and H. Leon Groves, Jr., for photographic processing, and Lisa Ramirez Bader for computer graphics. We appreciate the helpful reviews of the manuscript by Sherilyn Williams-Stroud and Joseph P. Smoot.

GEOLOGIC SETTING

The Paradox Basin in southeastern Utah and southwestern Colorado in the eastern part of the Colorado Plateau (fig. 1) is a structural and depositional basin that trends northwest-southeast adjacent to the southwest flank of the Uncompahgre Uplift. The depositional basin was asymmetrical in a northeast-southwest direction; it was deepest adjacent to the Uncompahgre Uplift and shallowed toward the shelf areas, which were toward the west, southwest, and south. The present sedimentary basin covers an area of approximately 11,000 mi² (28,500 km²), and its boundaries are defined by the limit of the halite deposits in the Paradox Formation of the Hermosa Group of Pennsylvanian age. The original maximum depositional thickness of the Paradox Formation was 5,000–6,000 ft (1,500–1,800 m) in the deepest part of the basin. The halite-bearing interval has been locally thickened to as much as 14,000 ft (4,300 m) in diapiric anticlines (Hite, 1968, p. 321).

Saline rocks of the Paradox Formation consist of 29 known halite-bearing evaporite cycles. Each cycle contains penesaline and siliciclastic rocks (interbeds) at the base and a halite bed, with or without potash, at the top. Individual halite beds are now 20–790 ft (6–240 m) thick near the basin

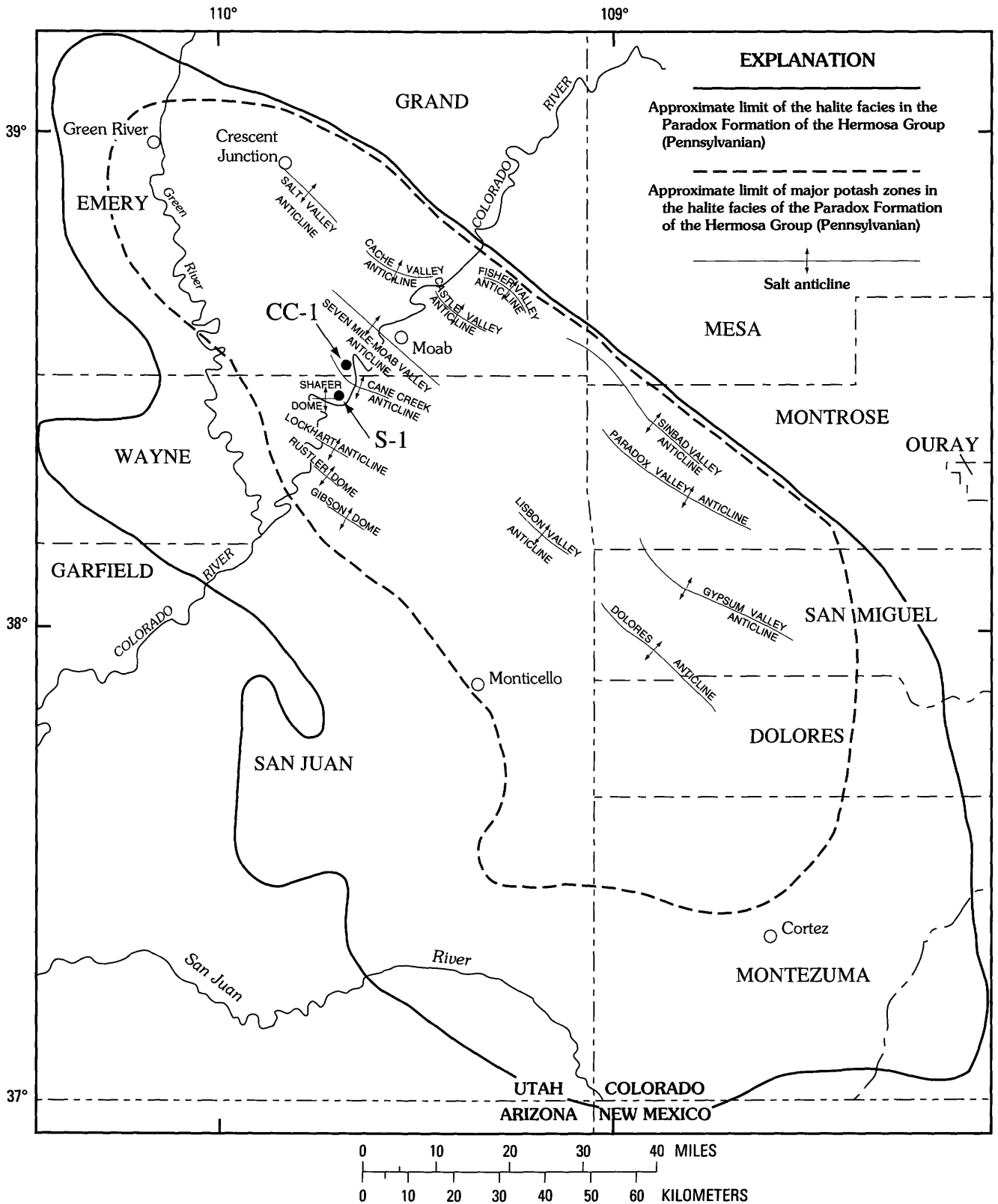


Figure 1. Limits of evaporite facies in the Paradox Formation of the Hermosa Group in the Paradox Basin, southwestern Colorado and southeastern Utah. Locations of Delhi-Taylor Oil Company Cane Creek No. 1 (CC-1) and Shafer No. 1 (S-1) core holes are also shown.

center (Hite 1983). Hite (1960) numbered the halite beds from 1 to 29 from top to bottom. Recent drilling, however, has shown that there are two younger, thin halite beds near the depocenter of the basin. These have not as yet been incorporated into the present numbering system.

The areal distribution of the evaporite facies reflects the asymmetry of the basin (fig. 1). The potash facies is best developed in areas that were the deepest parts of the basin adjacent to the Uncompahgre Uplift (unpub. data). The halite facies has a wider distribution and extends farther to the northwest, southwest, and southeast. The anhydrite facies extends beyond the halite facies, and the carbonate facies, both limestone and dolomite, extends onto the shelf areas beyond the edges of the basin (Hite and Buckner, 1981).

Rocks of the northeastern part of the Paradox Basin are folded into parallel anticlines and synclines that trend northwest-southeast. In the area of the thickest evaporites, the halite facies has flowed into the cores of the anticlines from the adjacent synclines. Anticlines closest to the Uncompahgre Uplift are diapiric, and large volumes of halite in the upper parts of their cores have been removed by dissolution. In anticlines farther from the uplift, the halite facies is conformable with overlying sedimentary rocks. This is the case for both the Cane Creek Anticline and Shafer Dome, from which the cores of this study were taken.

The Paradox Basin was formed in Pennsylvanian time in response to plate collisions that produced the Ouachita-Marathon orogeny (Kluth and Coney, 1981). The South American-African plate encountered the North American plate from the southeast starting in Late Mississippian to Early Pennsylvanian time. Major structural displacement occurred from Middle Pennsylvanian to Early Permian time. The major stresses of impact progressed from east to west, first in the Ouachita area, then in the Marathon Basin area (Ross, 1979). Structural deformation in the ancestral Rocky Mountains responded to the same east to west sequence. Coarse arkose flanking the ancestral Front Range is Early Pennsylvanian to Early Permian in age (Mallory, 1975), whereas arkose flanking the Uncompahgre Uplift is Late Pennsylvanian and Permian in age (Peterson and Hite, 1969).

Tectonism in and around the Paradox Basin reached a climax with major downwarping of the basin in Desmoinesian time. The major positive elements were the ancestral Front Range, the Uncompahgre Uplift, the Emery Uplift, the Piute positive element (Mallory, 1975), and the ancestral Kaibab and Zuni-Defiance Uplifts (Peterson and Hite, 1969). Except for the deeper water parts of the Paradox Basin, the surrounding areas were covered by shallow seas.

CORE DESCRIPTION

This study of evaporite cycles in the Paradox Basin is based on two cores: the Delhi-Taylor Oil Company Cane

Creek No. 1 and the Delhi-Taylor Oil Company Shafer No. 1. In these holes, which were drilled for potash, much of the upper part of the Paradox Formation was cored. These two core holes are located on nondiapiric salt anticlines where the stratigraphic sequence of the Paradox Formation is still well preserved. The two cores are described in Raup and Hite (1991a, b).

Hite (1960) and Hite and Buckner (1981) established stratigraphic correlation of the evaporite cycles in the Paradox Formation throughout the Paradox Basin. The correlations were based on distinctive geophysical log signatures of many of the penesaline and siliciclastic intervals (interbeds) within the evaporite sequence; these log signatures can be traced from one end of the basin to the other and from the evaporite facies in the center of the basin into the carbonate rocks on the shelf of the basin.

DELHI-TAYLOR OIL COMPANY CANE CREEK NO. 1

The Delhi-Taylor Oil Company Cane Creek No. 1 well was drilled near the crest of the Cane Creek Anticline, Grand County, Utah, in section 25, T. 26 S., R. 20 E. (fig. 1). The total depth of the hole was 2,805 ft (855 m), and the cored interval included four of the upper five evaporite cycles of the Paradox Formation (fig. 2). Coring started at a depth of 1,840 ft (561 m) in limestone of the Honaker Trail Formation, which overlies the Paradox Formation and is the upper formation of the Hermosa Group.

The rocks of cycle 1 are represented in this core hole by anhydrite, silty dolomite, black shale, and some limestone that overlie the halite bed of cycle 2. The halite bed of cycle 1 is present in the northeast part of the basin (depocenter) but is absent at this location.

The upper part of cycle 2 contains a bed of halite that is 171.3 ft (52.2 m) thick and is underlain by interbed units that are 110.2 ft (33.6 m) thick. The vertical distribution of the rock types in the interbeds is remarkably symmetrical and complete. The major rock types of this interval are anhydrite, silty dolomite, and black shale (Raup and Hite, 1991a). The basal anhydrite contains a thin unit of black shale.

The upper part of cycle 3 contains a bed of halite that is 133.8 ft (40.8 m) thick and is underlain by interbeds that are 106 ft (32.3 m) thick. Like cycle 2, these interbeds are vertically symmetrical with respect to lithology. The base of this interval is anhydrite, overlain successively by silty dolomite, black shale, silty dolomite, and anhydrite. A detailed log of these interbeds is illustrated in figure 5, and a detailed description is given later.

The halite bed at the top of cycle 4 is 179.5 ft (54.7 m) thick. It overlies interbeds that are only 37 ft (11.3 m) thick. In addition to being thin, this interval does not have the regular vertical symmetry of cycles 2 and 3. The lithologic units of these interbeds are thin and repetitious.

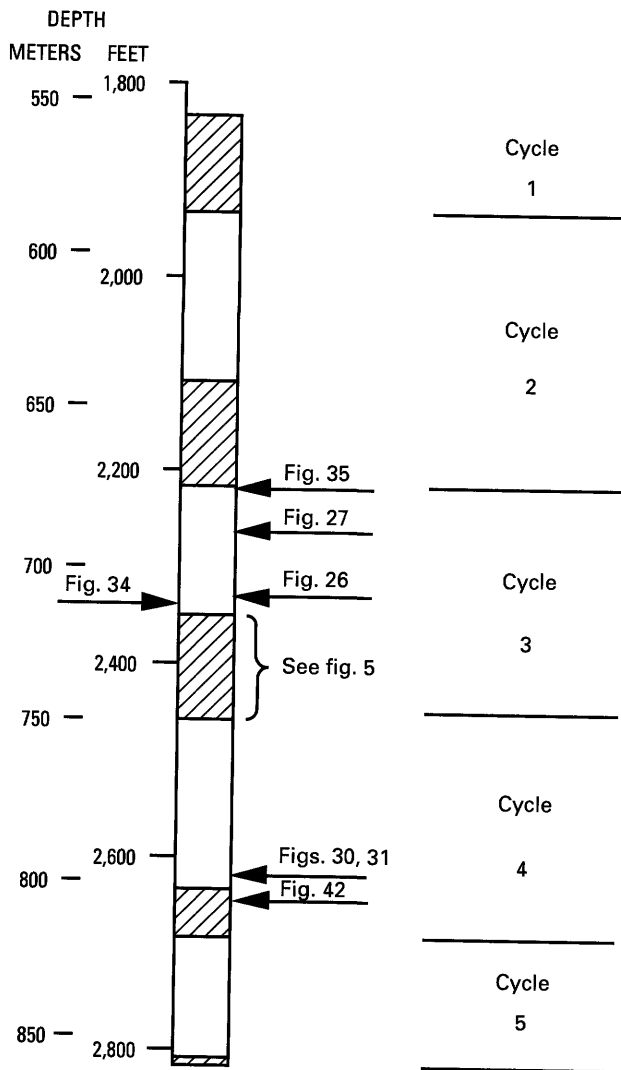


Figure 2. Schematic stratigraphy of Cane Creek No. 1 core hole. Penesaline and siliciclastic intervals (interbeds) between halite beds (nonpatterned) are indicated by a diagonal pattern. Locations of photographic figures are indicated by arrows; location of core hole shown in figure 1.

The halite bed of cycle 5 and only 1 m of anhydrite in the underlying interbed were drilled in this core hole. The halite bed is 127.3 ft (38.8 m) thick. A bed of sylvinitic (crystalline intergrowth of sylvite and halite), approximately 11.8 ft (3.6 m) thick, is near the top of this halite bed. The Texasgulf Corporation has been mining this potash deposit near Moab, Utah, since 1964.

DELHI-TAYLOR OIL COMPANY SHAHER NO. 1

The Delhi-Taylor Oil Company Shafer No. 1 well was drilled on the crest of Shafer Dome 14 mi (22.5 km) southwest of Moab, Utah, in section 15, T. 27 S., R. 20 E.,

San Juan County, Utah. It was drilled to a depth of 4,155.8 ft (1,266.7 m) through 11 of the 29 numbered evaporite cycles in the Paradox Basin (figs. 1, 3). Coring started at 2,160.1 ft (658.4 m) just above the halite bed of cycle 2. The halite bed of cycle 1 halite is absent in this part of the basin. No core was taken from just below the top of the halite bed of cycle 2 to about 30 ft (6.7 m) above the base of the halite bed in cycle 3 (fig. 3) (Rau and Hite, 1991b).

The interbeds of cycle 3 have the same very regular vertical symmetry as the same interval in the Cane Creek No. 1 core. A detailed correlation and comparison of this interval in both wells is presented later (fig. 5).

Both the halite bed and the interbeds in cycle 4 are thin, 29.8 ft (9.1 m) and 37 ft (11.3 m), respectively. The interbeds of cycle 4 are mostly silty dolomite; thin beds of anhydrite are at the top and bottom of the interbeds and a very thin black shale is in the middle.

The halite bed of cycle 5 is 213.9 ft (65.2 m) thick and contains widely disseminated crystals of sylvite. Although there is no economic concentration of sylvite in cycle 5 at this locality as there is at Cane Creek No. 1, the total interval of sylvite-mineralized rock is thicker.

The halite bed of cycle 6, one of the thickest halite beds in the upper part of the Paradox Formation, is 312 ft (95.1 m) thick. The underlying interbeds, on the other hand, are only 23 ft (7 m) thick and contain only anhydrite and dolomite. A zone of sylvinitic near the top of the halite bed is approximately 20 ft (6 m) thick.

Cycle 7 contains a halite bed that is 99.1 ft (30.2 m) thick. The interbeds at the base of the cycle are only 9.8 ft (3 m) thick and are mostly anhydrite with a thin dolomite in the middle.

Cycle 8 is similar to cycle 7 in that the interbeds are composed only of anhydrite and dolomite. The halite bed is 69.9 ft (21.3 m) thick, and the interbeds are 46.9 ft (14.3 m) thick.

The halite bed of cycle 9 contains a zone of sylvinitic near its top that is approximately 19.7 ft (6 m) thick. The halite bed is 157.8 ft (48.1 m) thick, and the underlying interbeds are 35.1 ft (10.7 m) thick. The bottom two-thirds of the interbeds is dolomite, and the upper third is anhydrite. A thin bed of black shale is in the upper part of the dolomite.

The halite bed of cycle 10 is very coarsely crystalline in its upper part, and it contains several thin zones of anhydrite-halite pseudomorphs after gypsum. This halite bed is 134.8 ft (41.1 m) thick, and the underlying interbeds are 36 ft (11 m) thick. The interbeds consist mainly of anhydrite and dolomite and contain three thin zones of black shale near the top.

The halite bed of cycle 11 is only 25.9 ft (7.9 m) thick. It is underlain, however, by thick interbeds that contain two relatively thick black shale beds and some relatively thin black shale beds. Because the halite of cycle 12 is not present in this core, it is probable that part of these interbeds represents cycle 12.

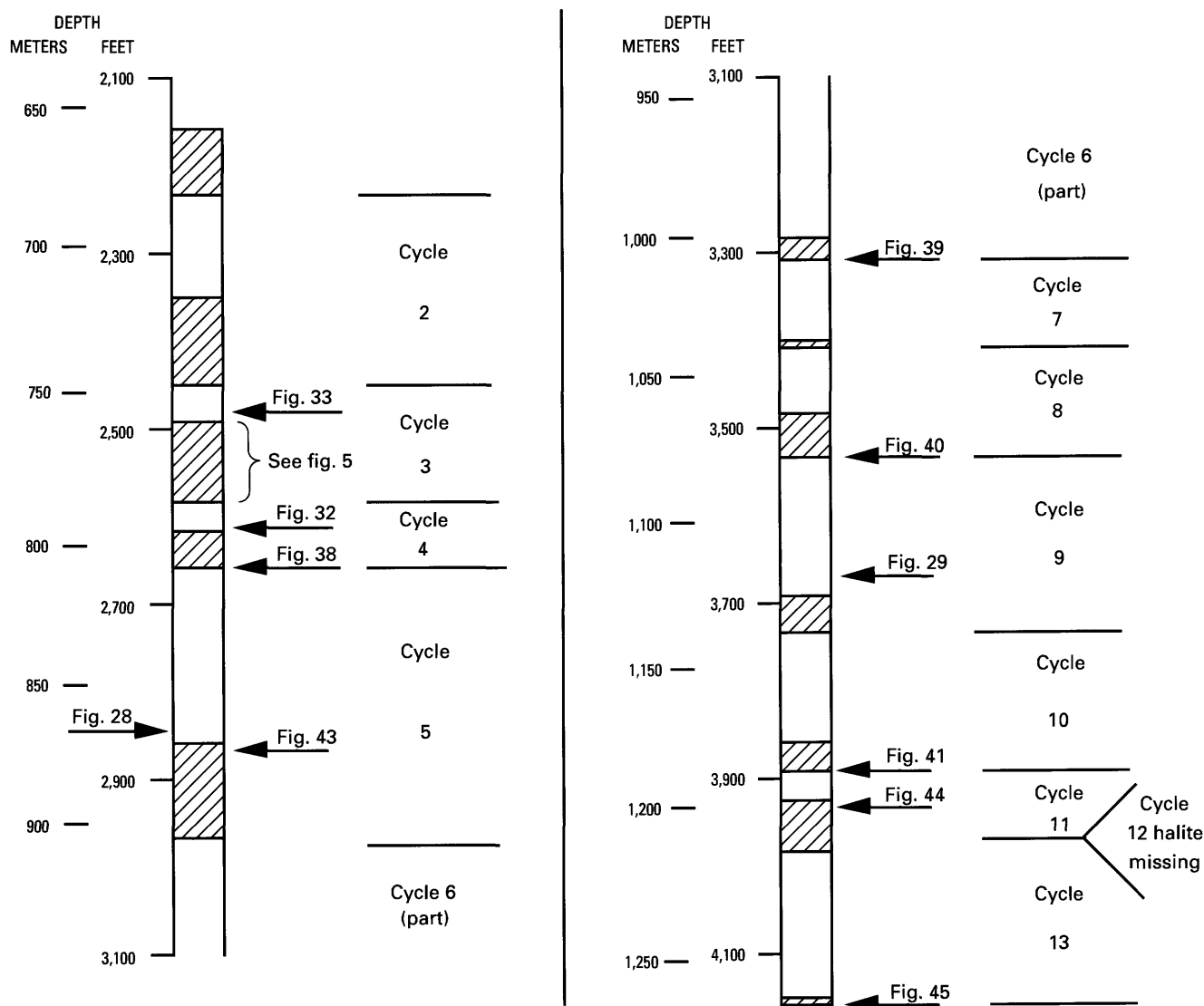


Figure 3. Schematic stratigraphy of Shafer No. 1 core hole. Penesaline and siliciclastic intervals (interbeds) between halite beds (nonpatterned) are indicated by diagonal pattern. Locations of photographic figures are indicated by arrows; location of core hole shown in figure 1.

The halite bed of cycle 13 and a few feet of underlying anhydrite constitute the base of this core hole. This halite bed, which is 169.9 ft (51.8 m) thick, contains thin beds and disseminated crystals of sylvite scattered throughout, except for a few meters at the base. Small nodules of kieserite ($MgSO_4 \cdot H_2O$) are in a 16.4-ft (5 m) -thick zone near the middle of the halite bed.

EVAPORITE CYCLES

Each of the evaporite cycles in the upper part of the Paradox Formation of the Hermosa Group in both the Cane Creek and Shafer cores contains a halite bed and an underlying sequence of penesaline and siliciclastic rocks that we

collectively refer to as interbeds (figs. 2-4). The cycles are separated by erosional or dissolution unconformities that are characterized by sharp knife-edge contacts (Hite, 1970; Hite and Buckner, 1981; Raup and Hite, 1991a, b).

Most of the interbeds are made up of anhydrite, dolomite, and organic-carbon-rich carbonate shale (black shale). Some interbeds contain primarily anhydrite and dolomite and little or no black shale. Each of the interbeds has anhydrite at the top and bottom, and most contacts within the interbeds are gradational.

Of the 11 cycles available for study in the Cane Creek and Shafer cores, the most perfectly developed, in terms of lithologic representation and distribution, are cycles 2 and 3. The interbeds of these two cycles are vertically symmetrical and comprise a sequence of anhydrite, silty dolomite, black

shale, dolomite, and anhydrite. Figure 4 illustrates the stratigraphic sequence in cycle 2.

A typical cycle starts at the base of the lower anhydrite at a disconformity at the top of the underlying halite bed. As we discuss later, we believe that the cycle is initiated by an abrupt rise in sea level and an influx of sea water into the basin (letter X, fig. 4). The lower part of the interbeds, therefore, is termed the transgressive phase because of rising sea level. We believe that sea level reached a maximum during deposition of the middle of the black shale (letter Y) and then began to drop. Thus, we consider the rock types in the upper part of the cycle (Y to Z) to be regressive.

It is probable that the cycles in the lower part of the Paradox Formation were deposited in relatively deep water in a basin that had subsided before evaporite deposition started. The rapid rate of evaporite deposition, however, quickly overtook basin subsidence, and the basin rapidly filled with evaporites in a manner described for other evaporite basins (Borchert and Muir, 1964; Wardlaw and Schwerdtner, 1966; Schmalz, 1969).

LITHOLOGIC CHARACTERISTICS OF CYCLES 2 AND 3 OF THE PARADOX FORMATION

The lithology described for cycle 2 (fig. 4) (Hite and Buckner, 1981) and cycle 3 (fig. 5) is very regular with respect to vertical distribution and representation of the evaporite rock types. Each of the cycles is bounded top and bottom by a solution disconformity, and each has a sequence, from base upward, of anhydrite, silty dolomite, organic-carbon-rich carbonate shale (black shale), dolomite, anhydrite, and halite. All of the contacts within the interbeds between these rock types are conformable, and most are gradational.

The lithologic sequences of cycles 2 and 3 (figs. 4 and 5, respectively) are almost identical. Hite and Buckner (1981) described and interpreted the depositional history of cycle 2. Most of the lithologic detail presented herein is from cycle 3, but lithologic features of both cycles are presented and interpreted. Some general characteristics of the major rock types are included from descriptions of other cycles (Raup and Hite, 1991a, b).

Semiquantitative mineralogy of the various rock types in the interbeds of cycles 2 and 3 in the Cane Creek No. 1 core, as determined by X-ray diffraction, is illustrated by histograms for the minerals halite, anhydrite, calcite, dolomite, quartz, plagioclase, orthoclase, and clay and mica (fig. 6) (Raup and Hite, 1991a). The quantities of the minerals were determined by comparing major peak heights of minerals in the samples with peak heights of prepared standards.

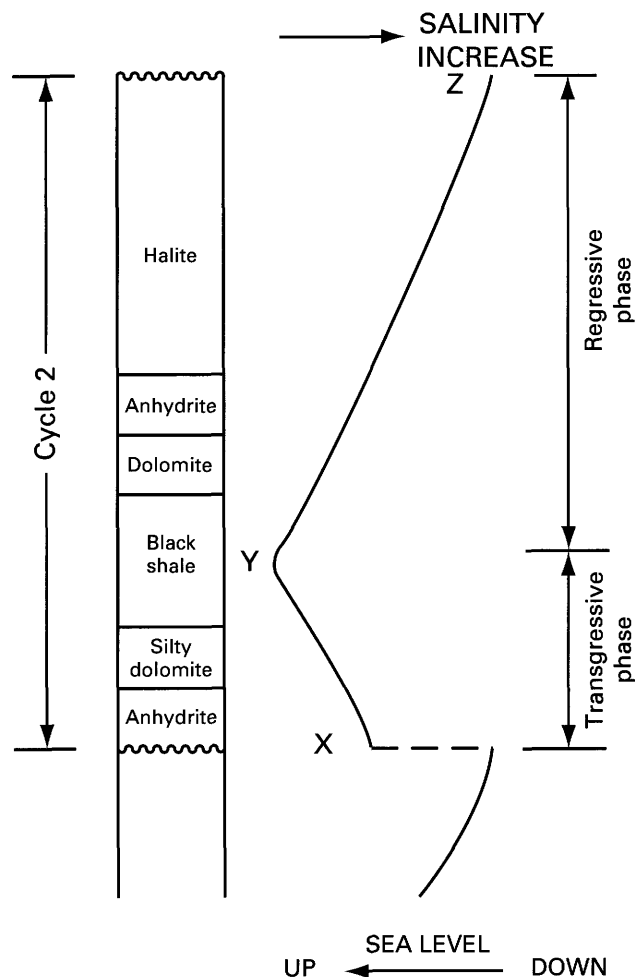


Figure 4. Stratigraphy of cycle 2 facies in Cane Creek No. 1 core. Curve shows relative sea level and salinity during deposition of each facies. Points X, Y, and Z (referred to in text) are important positions in the salinity cycle. Location of core hole shown in figure 1. Modified from Hite and Buckner (1981).

INTERBEDS

ANHYDRITE (TRANSGRESSIVE)

The lower anhydrite unit in cycle 3 overlies the halite bed of cycle 4 with a very sharp, knife-edge contact (solution disconformity) in both the Cane Creek and Shafer cores (figs. 7, 8). The anhydrite rock is composed primarily of the mineral anhydrite and locally minor amounts of interspersed dolomite. Other minor constituents include quartz, mica, clay minerals, and pyrite. The basal part of this anhydrite unit is very fine grained and laminated. The laminae average 1–3 mm thick and consist of light-gray to dark-gray or tan layers. The darker layers are colored by accumulations of organic matter. The laminated interval in the Cane Creek core is about 4.4 ft (1.3 m) thick. The laminated interval is overlain by nodular anhydrite (figs. 9–12). This nodular interval in the Cane Creek core is 8.6 ft (2.6 m) thick.

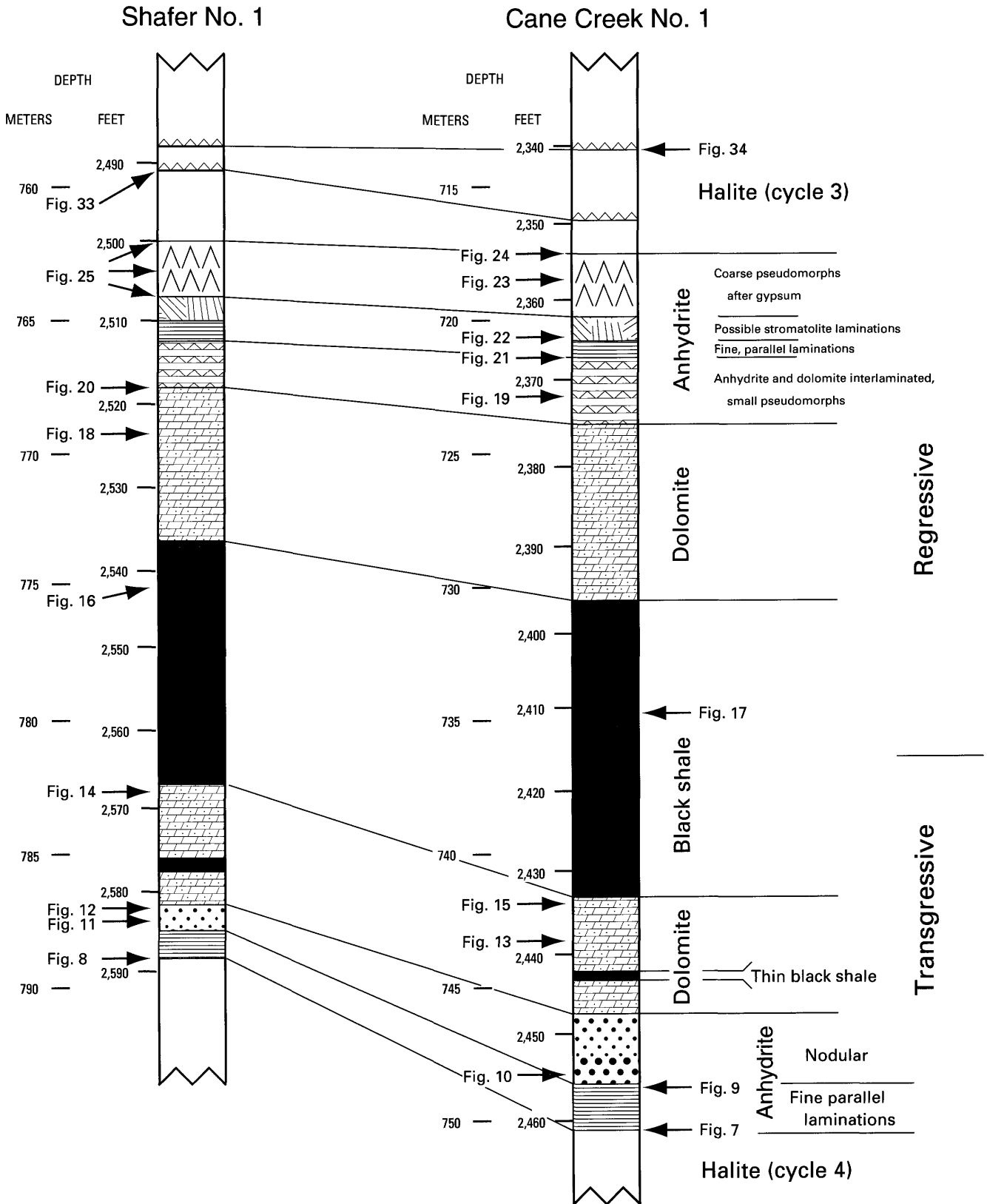
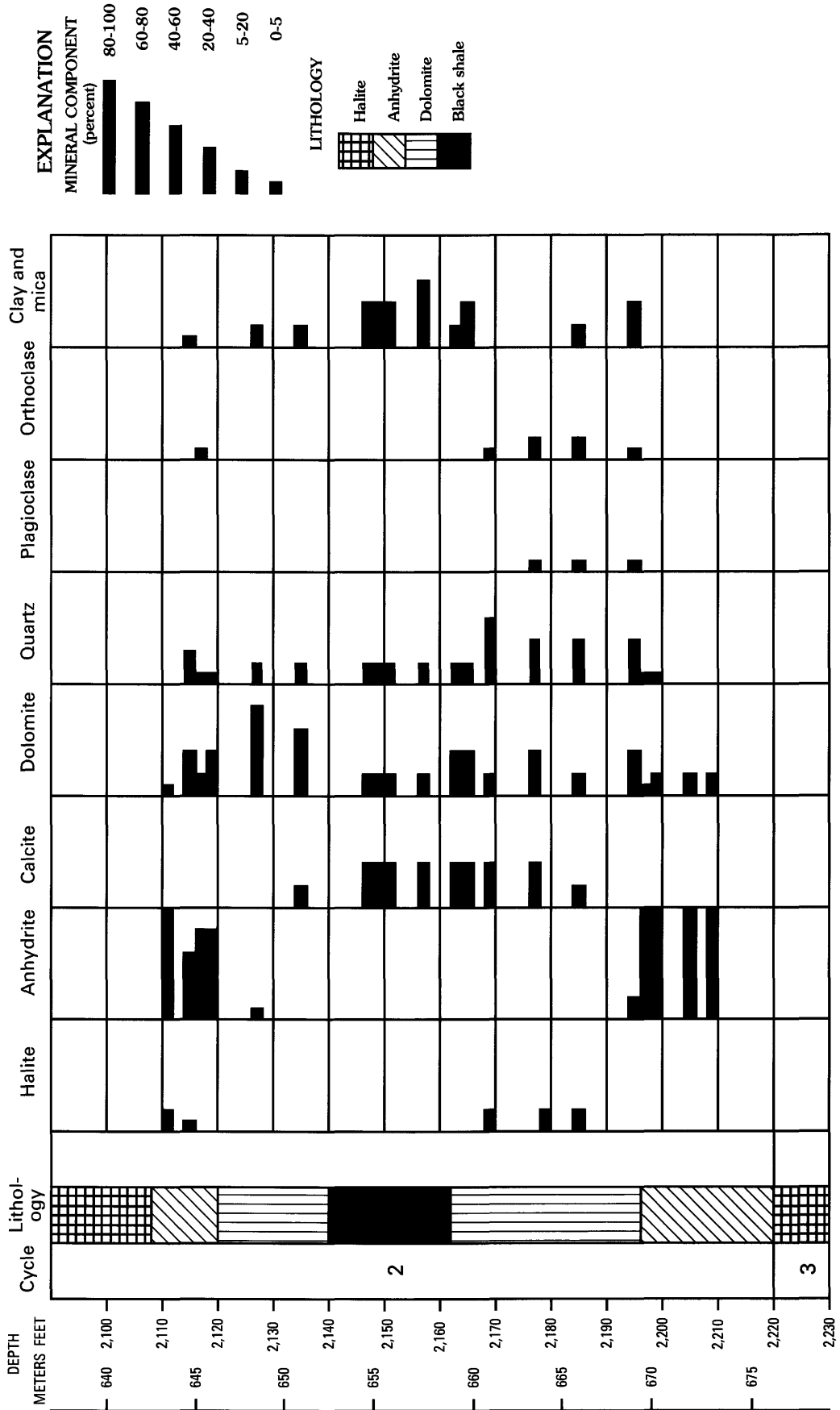


Figure 5. Correlation of lithologic units in Shafer No. 1 and Cane Creek No. 1 cores in penesaline and siliciclastic rocks (interbeds) and lower part of halite bed near base of cycle 3 (see figs. 2, 3). Base of transgressive anhydrite at bottom of interbeds is in knife-edge contact with underlying halite bed (cycle 4). Top of regressive anhydrite, at top of interbeds, contains coarse pseudomorphs of anhydrite and halite after gypsum; pseudomorphs are gradational with overlying halite bed. Locations of photographic figures are indicated by arrows; locations of core holes are shown in figure 1.

EVOLUTION OF SEDIMENTARY BASINS—PARADOX BASIN



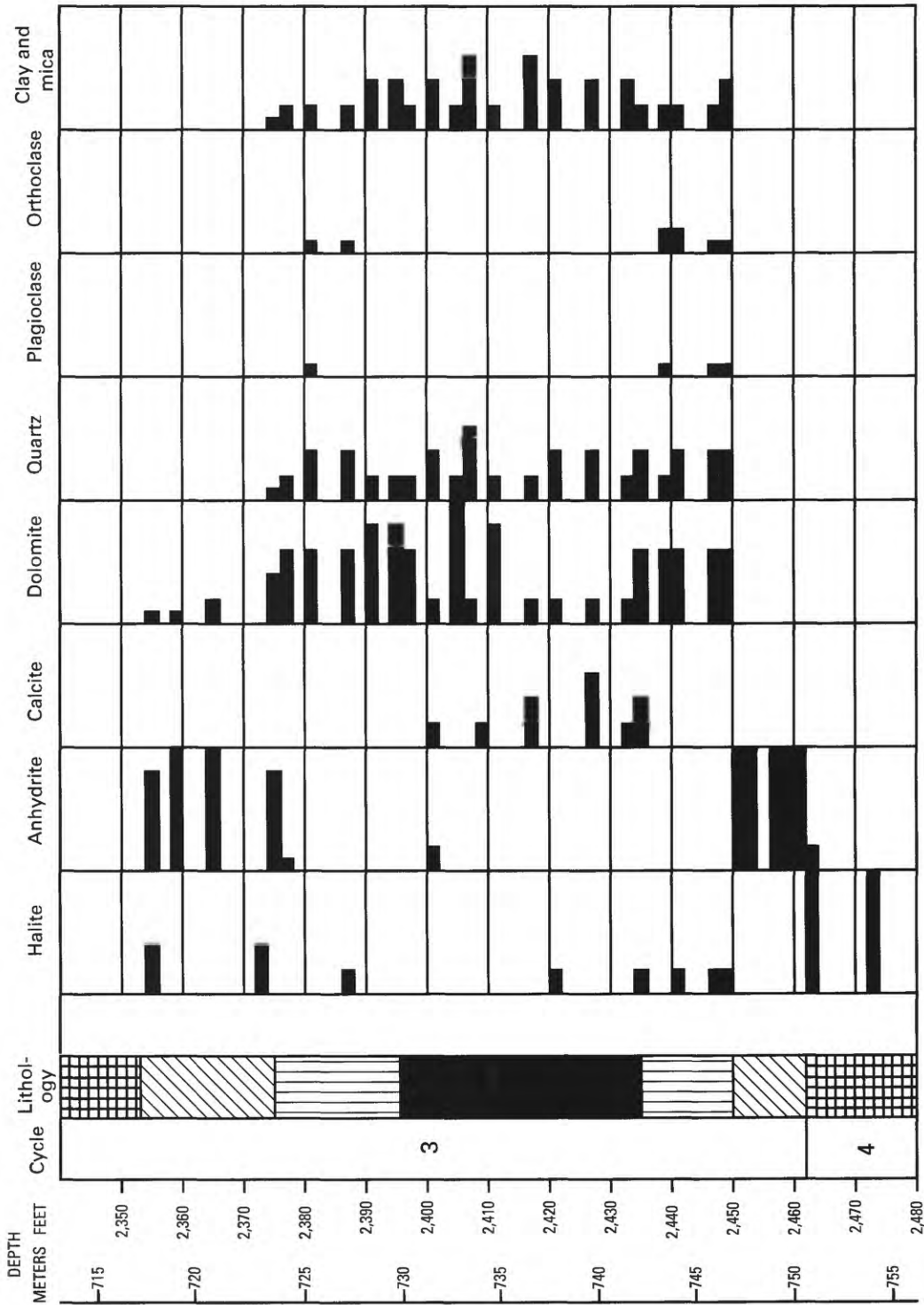


Figure 6 (above and facing page). Mineral composition of penesaline and siliciclastic intervals in Cane Creek No. 1 core as determined by X-ray diffraction. Quantities of minerals were determined semiquantitatively by comparing major peak heights of minerals in samples with peak heights of prepared standards. Lengths of histogram bars represent ranges in amounts of mineral components (Raup and Hite, 1991a). Location of core hole shown in figure 1.



Figure 7. Photograph of polished surface of core from Cane Creek No. 1 core, depth 2,460.5 ft (750 m), illustrating sharp contact (arrow) between overlying laminated anhydrite at base of interbeds at base of cycle 3 and halite bed at top of cycle 4. This part of halite bed 4 contains small pseudomorphs of halite and anhydrite after gypsum. Location of core shown in figure 5.



Figure 8. Photograph of polished surface of core from Shafer No. 1 core, depth 2,588 ft (788.8 m), illustrating sharp contact (arrow) between overlying, finely laminated anhydrite at base of interbeds at base of cycle 3 and halite bed at top of cycle 4. Location of core shown in figure 5.



Figure 9. Photograph of polished surface of core from Cane Creek No. 1 core, depth 2,456.5 ft (748.7 m), illustrating laminated transgressive anhydrite grading upward into nodular anhydrite near base of cycle 3. Location of core shown in figure 5.

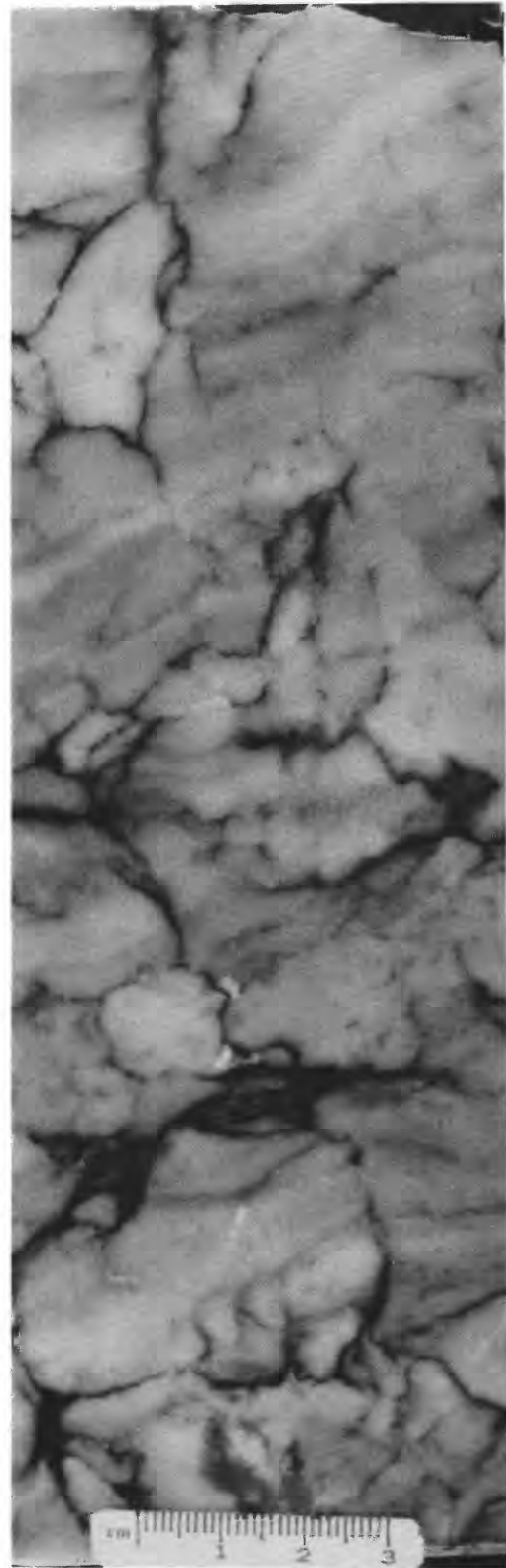


Figure 10. Photograph of polished surface of core from Cane Creek No. 1 core, depth 2,455.3 ft (748.4 m), illustrating nodular transgressive anhydrite in lower part of cycle 3. This is classic chicken-wire texture of nodular anhydrite. A faint remnant layering is visible through nodules. Location of core shown in figure 5.

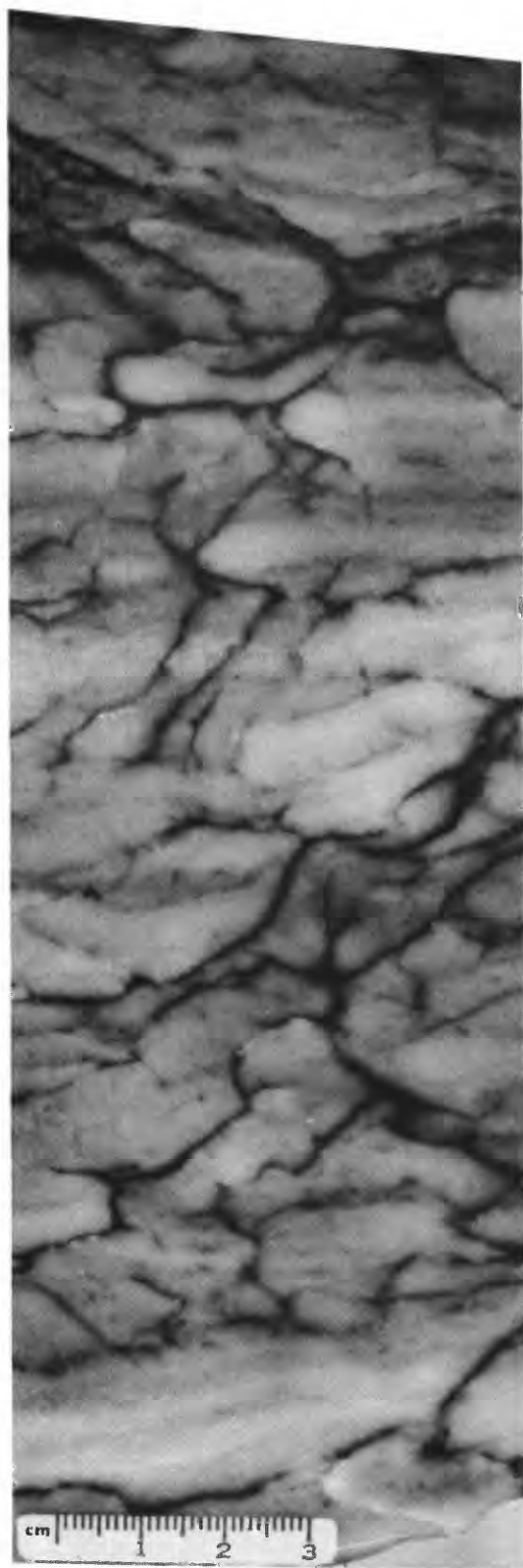


Figure 11. Photograph of polished surface of core from Shafer No. 1 core, depth 2,583.5 ft (787.4 m), illustrating nodular transgressive anhydrite in lower part of cycle 3. Remnant horizontal layering is visible through nodules. Location of core shown in figure 5.

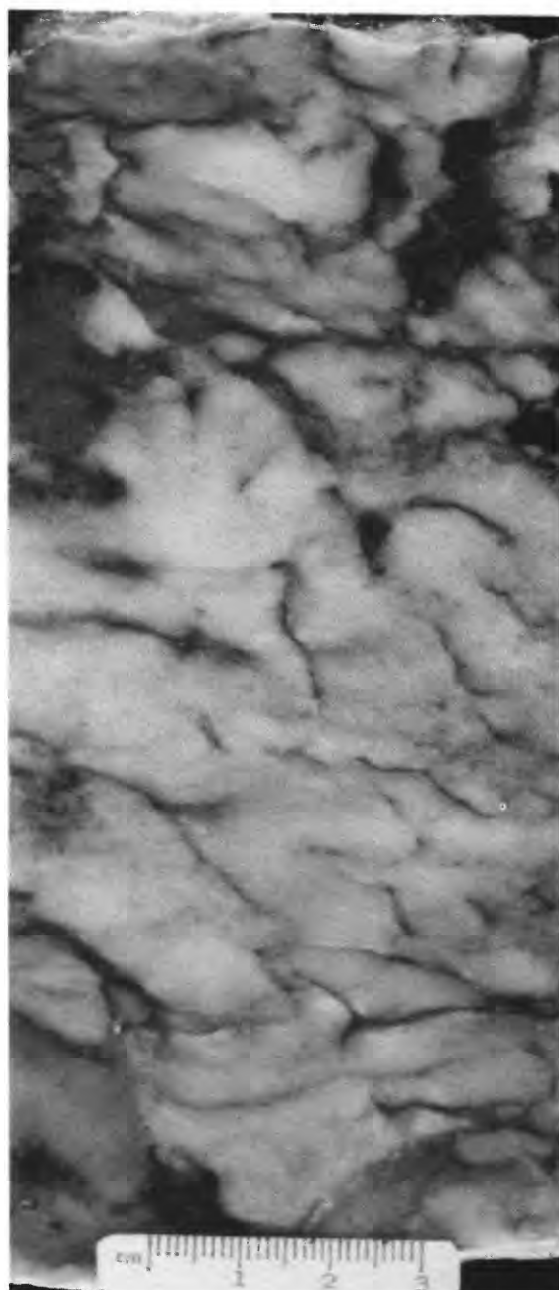


Figure 12. Photograph of polished surface of core from Shafer No. 1 core, depth 2,581.5 ft (786.8 m), illustrating nodular transgressive anhydrite in lower part of cycle 3. Location of core shown in figure 5.

The disconformities at the base of cycles 2 and 3, as well as those of all of the other cycles in the upper part of the Paradox Formation, are thought to result from an abrupt rise in sea level as indicated by the sea-level curve in the center of the diagram (fig. 4). This rise in sea level resulted in an inflow of sea water that caused an overall lowering of brine salinities in the basin and dissolution of the upper part of the halite bed of the preceding cycle. The character of the dissolution surfaces could be observed in the underground

workings of the Texasgulf potash mine near Moab, Utah. Two photographs of these underground exposures are illustrated in a paper by Hite (1970, p. 56, 57). The transgressive phase of deposition, from point X to point Y in figure 4, is considered to have occurred during a rise in sea level. The anhydrite of this phase, which is laminated in the lower part of cycle 3 and nodular in the upper part (fig. 5), was probably deposited as a result of a new influx of calcium and sulfate into the basin from the open ocean. The laminated anhydrite (possibly originally gypsum) would have been deposited during the early stages of influx when the salinity of the brines in the basin was still very high, and it may have precipitated from the incoming brine as that brine mixed with brines of higher salinity that were already in the basin (Raup, 1982).

The upward progression of laminated anhydrite to nodular anhydrite may be related to the reduction in brine salinity as conditions approached those for the deposition of the dolomite. The nodular anhydrite is probably a diagenetic texture that resulted from recrystallization of laminated anhydrite in the bottom muds in the presence of brines of lower salinity. Traces of laminations through the nodules indicate that the nodular anhydrite (fig. 11) was originally laminated and that the nodular texture is a secondary feature. The transgressive anhydrite in the interbeds of cycles 4, 5, 6, 8, and 10 also exhibits laminated textures grading to nodular textures as it approaches rock types that were deposited under less saline conditions. These examples also indicate that the changes in texture from laminated to nodular anhydrite are probably related to changes from higher to lower salinity.

Since the discovery of anhydrite nodules in the modern sediments along the Trucial Coast of the Arabian Gulf in what is considered a classic example of the sabkha depositional environment (Kinsman, 1966; Butler, 1969), researchers have been quick to interpret any nodular anhydrite as having formed in a sabkha setting. Dean and others (1975), in their paper on the sedimentological significance of nodular and laminated anhydrite in the Delaware Basin, made a good case for the diagenetic origin of nodular anhydrite regardless of original depositional setting. Dean and others (1975) and Dean and Anderson (1978, 1982) described cycles in the Permian Castile Formation of Texas and New Mexico in which laminated anhydrite grades upward into nodular anhydrite that is overlain by halite. In this sequence, the nodular anhydrite probably formed in an environment of increasing salinity rather than the decreasing salinity sequence of the Paradox cycles. Like the evaporite cycles of the Castile Formation, the Paradox cycles probably were deposited by subaqueous processes, and the nodular anhydrite in the middle of this sequence is part of these processes. The nodular anhydrite in the Paradox Basin evaporites most likely formed as the result of diagenesis that occurred early in the depositional process or at some later time. The original calcium sulfate precipitation may have been gypsum, and the

nodules may have formed when the gypsum was converted to anhydrite.

SILTY DOLOMITE (TRANSGRESSIVE)

The anhydrite is overlain by silty dolomite above a contact that in both cores is abrupt. In general the dolomitic rocks are composed of mainly dolomite, varying significant amounts of quartz, calcite, anhydrite, clay, and mica, and minor amounts of orthoclase, plagioclase, and some halite. All of the constituents of the dolomitic rocks are fine to very fine grained. The rocks have a sugary to earthy texture and are medium to light tannish gray. The transgressive dolomite in cycle 3 has a fine-grained sugary texture (figs. 13, 14) that is due in part to silt-sized sucrosic dolomite crystals and in part to very well sorted quartz grains of about the same size. These rocks have indistinct and occasional disrupted bedding. Some irregularities in the bedding may be due to bioturbation. This dolomite in cycle 3 in the Cane Creek core is 14.4 ft (4.4 m) thick. The lower half of this dolomite, in both cores, contains a thin interval of black shale (see fig. 5).

The transgressive dolomite precipitated as an influx of sea water continued to cause a further drop in basin salinities and the basin brines were enriched in the HCO_3^- ion. The fine-grained sucrosic texture of the dolomite in the Paradox interbeds probably is the result of early diagenetic dolomitization or of primary precipitation. Reduced dissolved sulfate in the basin brines, caused by bacterial reduction (Baker and Kastner, 1981) and (or) precipitation of reaction calcium sulfate as a result of dolomitization (Hite, 1985), could have contributed to conditions necessary for the precipitation of primary dolomite. Subtle textural and physical properties of chemical sediments, however, are subject to alteration through geologic time (Hardie, 1987).

This transgressive dolomite contains a high percentage (as much as 40 percent) of detrital quartz and some feldspar, and the grain size of this material is about the same as that of the sucrosic dolomite (figs. 6, 15). Much of the quartz and feldspar and possibly much of the dolomite may have been transported to the site of deposition by density currents similar to the mechanism proposed by Harms (1974) for parts of the Permian Brushy Canyon Formation in the Delaware Basin. The currents may have acquired clastic material as the shoreline advanced through the arkosic fan deltas adjacent to the Uncompahgre Uplift during rising sea level. The high degree of sorting of the quartz may be the result of winnowing of the material during current transport. Hite and Buckner (1981) believed that the remarkably well sorted material indicates that deposition may have been from turbidity currents that flowed across the basin on dense bottom-basin brines. The high degree of sorting of the quartz also suggests the possibility of an eolian origin. Further petrographic study on a regional scale would improve our understanding of the origin of these rocks.



Figure 13. Photograph of segment of Cane Creek No. 1 core, depth 2,438 ft (743.1 m), illustrating typical transgressive silty dolomite in lower part of cycle 3. This quartz-rich carbonate may have been deposited by a combination of density currents and chemical precipitation. Location of core shown in figure 5.

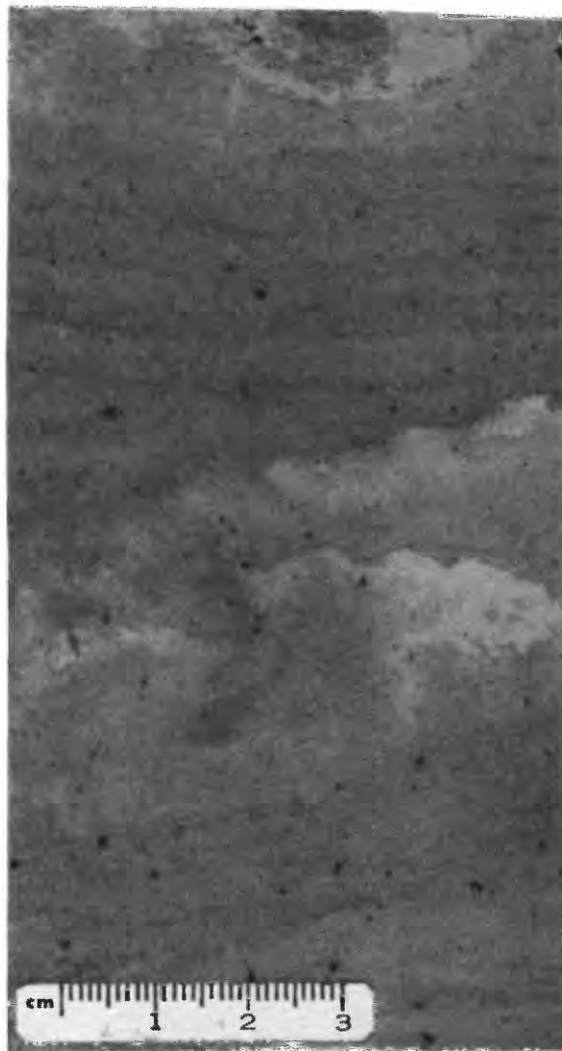


Figure 14. Photograph of polished surface of core from Shafer No. 1 core, depth 2,569 ft (783.0 m), illustrating typical transgressive silty dolomite in lower part of cycle 3. Faint laminations are marked by concentrations of organic matter. Black spots are very small nodules of organic matter and pyrite. Location of core shown in figure 5.

BLACK SHALE

The transgressive dolomite is overlain by organic-carbon-rich carbonate shale (black shale) (figs. 5, 16) that comprises the middle lithologic unit in these sets of interbeds. The black shale of the Paradox Formation consists mainly of dolomite, calcite, quartz, clay minerals, and mica and minor amounts of pyrite and some sphalerite (fig. 6). Samples taken from different cycles in both cores have almost identical mineral compositions. In cycle 3 of the Cane Creek core the contact between the underlying dolomite and the black shale is gradational, but in the Shafer core it is abrupt. This shale interval, referred to as the "Gothic shale" by industry, is 36.5 ft (11.1 m) thick in the Cane Creek core

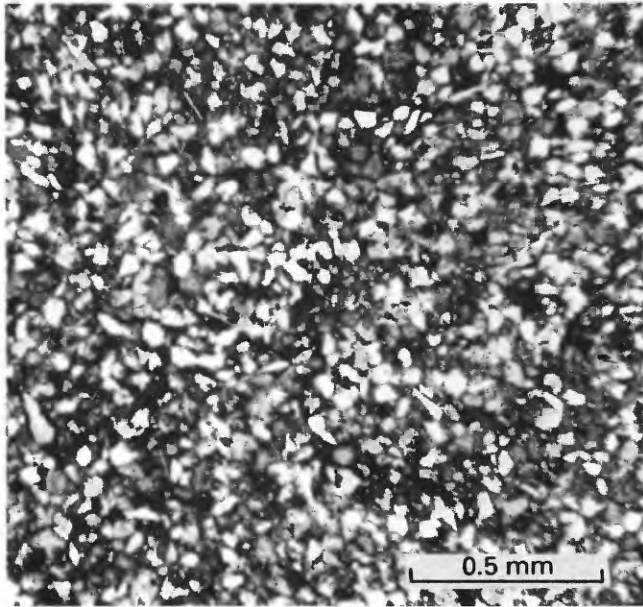


Figure 15. Photomicrograph of transgressive dolomite from Cane Creek No. 1 core, depth 2,433.5 ft (741.7 m); crossed nicols. Most of white, clear grains are quartz; cloudy gray grains are dolomite. Sample contains about 40 percent quartz. Location of core shown in figure 5.

and is dark gray to jet black. Its mineral components are fine-silt to clay sized and include dolomite, calcite, and quartz and minor amounts of feldspar, illite, and other clay minerals (fig. 6). Fine silt-sized quartz is abundant in some intervals in amounts of as much as 40 percent (fig. 17). The carbonate content is 20–30 percent (Hite, 1970). The total organic carbon content in the black shale of cycle 3 is 2–3 percent in the Shafer core (Hite and others, 1984, p. 264). Black shale in the interbeds of other cycles in the Paradox Basin contains organic matter in amounts from 0.5 to 13 weight percent (Hite and others, 1984). A few broken shell fragments, some small intact shells, and occasional conodonts indicate some biological activity.

The black shale was probably deposited during the time of highest sea level within each cycle when the salinity of the brines in the basin was lowest. The organic matter was probably derived from both marine and continental sources, as well as from algae and bacteria that flourished within the basin, and was preserved by residual, dense, relatively high salinity, anoxic brines that covered the basin floor. The siliciclastic components may have been deposited by density currents similar to those during deposition of the silty dolomite interval described earlier, but it is possible that a significant amount may have an eolian origin. An extensive discussion concerning the composition and origin of these unusual rocks is given in a paper by Hite and others (1984).

The upper part of the cycle 3 interbeds is interpreted as having been deposited during a lowering of sea level and is thus considered to be the regressive phase. The lowering of



Figure 16. Photograph of polished surface of core from Shafer No. 1 core, depth 2,542 ft (774.8 m), illustrating typical interval of organic-carbon-rich carbonate shale (black shale) near middle of interbeds in cycle 3. Location of core shown in figure 5.

sea level and the accompanying rise in salinity in the basin started sometime during deposition of the black shale as indicated at point Y on figure 4.

DOLOMITE (REGRESSIVE)

The black shale is overlain by a dolomite (fig. 18) that, like the transgressive dolomite, has a sugary texture. The contact between these rock types is gradational in the Cane Creek core and abrupt in the Shafer core. In the Cane Creek core this dolomite unit is 21 ft (6.4 m) thick. This regressive dolomite has a blotchy texture as a result of included organic matter and small clots of pyrite. Occasional zones of disrupted bedding may be the result of bioturbation.

The regressive dolomite was deposited at a time when basin salinities were rising. It contains somewhat less siliciclastic material than the transgressive dolomite, especially in cycle 2 (fig. 6), possibly because less clastic material may

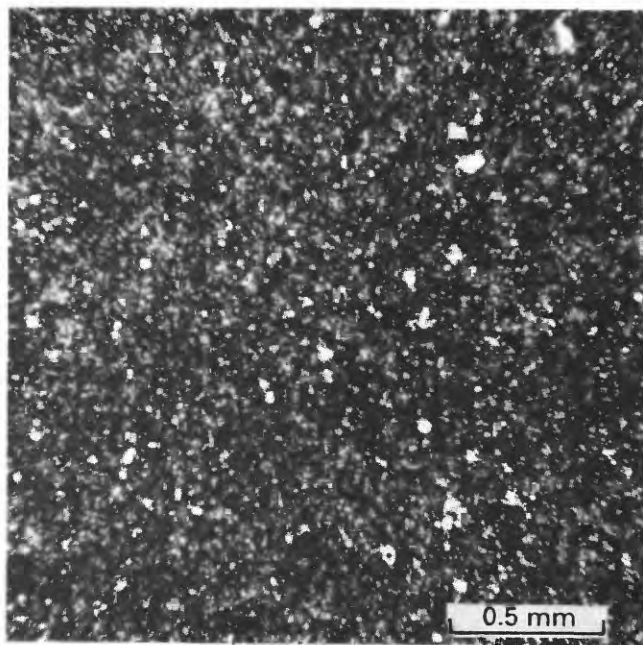


Figure 17. Photomicrograph of black shale from Cane Creek No. 1 core, depth 2,410.5 ft (734.7 m); crossed nicols. Sample contains about 15 percent very fine grained, silt-sized quartz. Location of core shown in figure 5.

have been available near the basin edges during the regressive phase of the cycle and because much of the available material would have been mobilized during the transgressive phase. Rainfall over the highland areas may also have been lower during this phase in the cycle, and therefore flooding from the land was less.

The transgressive dolomite, the black shale, and the regressive dolomite in cycles 2 and 3 contain abundant silt-sized siliciclastic material, mostly quartz. The other rock types of the cycles, anhydrite and halite, contain very little quartz. Rates of sedimentation of the different rock types may account, in large part, for these differences. If siliciclastic material entered the basin at an almost constant but slow rate, either by density currents from the shoreline or by wind, it would accumulate in greater amounts within the chemical sediments that precipitated the slowest. Hite and Buckner (1981, p. 157) showed that the dolomite and black shale were deposited, in general, at rates lower than the anhydrite and halite. This difference in deposition rates may account, at least in part, for the distribution of the siliciclastic material in these rocks.

Between the regressive dolomite and the overlying anhydrite is a transition zone of interbedded dolomite and anhydrite (fig. 5) that contains numerous thin layers of small pseudomorphs of anhydrite after gypsum (figs. 19, 20). In the Cane Creek core this transitional interval is 8.8 ft (2.7 m) thick. The increase in amount of anhydrite (gypsum) and the presence of bottom-growth crystals are indicative of rising salinity of the brines in the basin.



Figure 18. Photograph of polished surface of core from Shafer No. 1 core, depth 2,523.5 ft (769.2 m), illustrating an interval of regressive dolomite in upper part of interbeds in cycle 3. Blotches are composed of organic matter, pyrite, quartz, and minor halite. Location of core shown in figure 5.

ANHYDRITE (REGRESSIVE)

Anhydrite having a variety of textures overlies the dolomite-anhydrite transition zone. Laminated texture in the lower part of this anhydrite unit probably resulted from primary precipitation from the brine column as may also have occurred in the transgressive anhydrite (fig. 5). Extremely fine and wavy laminations in part of the unit may be the result of anhydrite replacement of carbonate algal mats (fig. 21). This interval in the Cane Creek core is 2 ft (0.6 m) thick. Above the finely laminated anhydrite is a 3-ft (1 m) -thick zone of anhydrite that contains clasts of extremely finely laminated anhydrite. This zone, too, could possibly be a replacement of algal mat structures (fig. 22). If this finely laminated anhydrite was originally produced by algal deposition, the zone of deposition must have been within the photic zone (water depth less than 80 m). Cycle 3 is in the upper part of the Paradox Formation and thus was probably deposited in relatively shallow water during the later stages

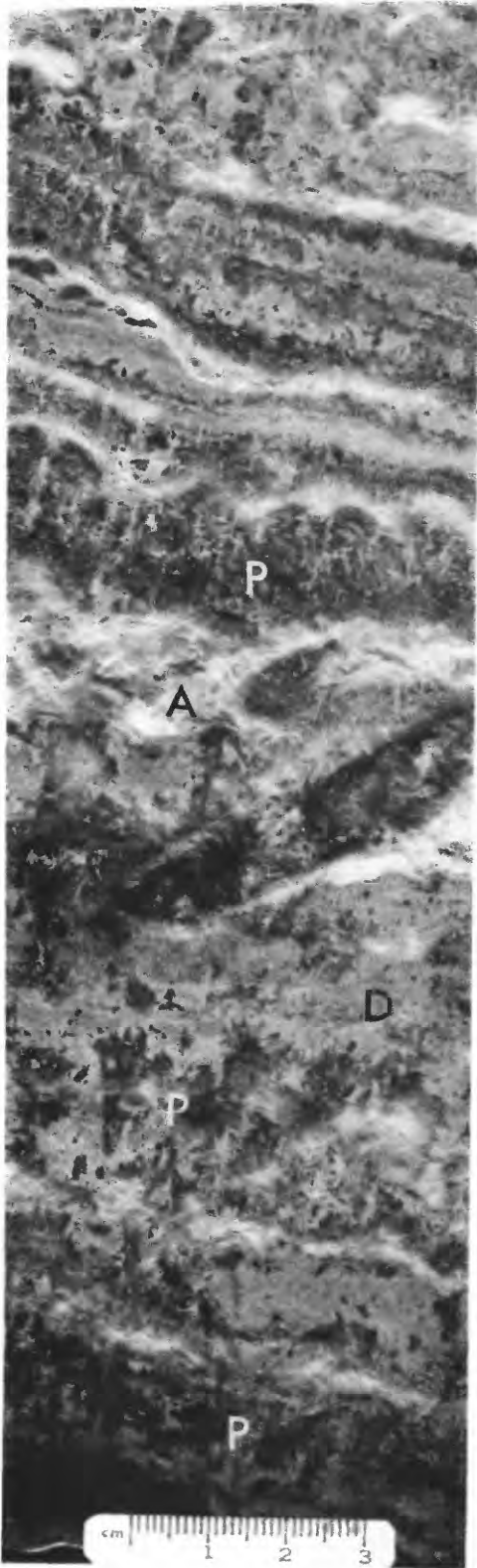


Figure 19. Photograph of polished surface of core from Cane Creek No. 1 core, depth 2,372 ft (722.0 m), illustrating an interval of interbedded dolomite (D) and anhydrite (A) that contains pseudomorphs (P) after bottom-growth gypsum in regressive phase in upper part of interbeds in cycle 3. Location of core shown in figure 5.

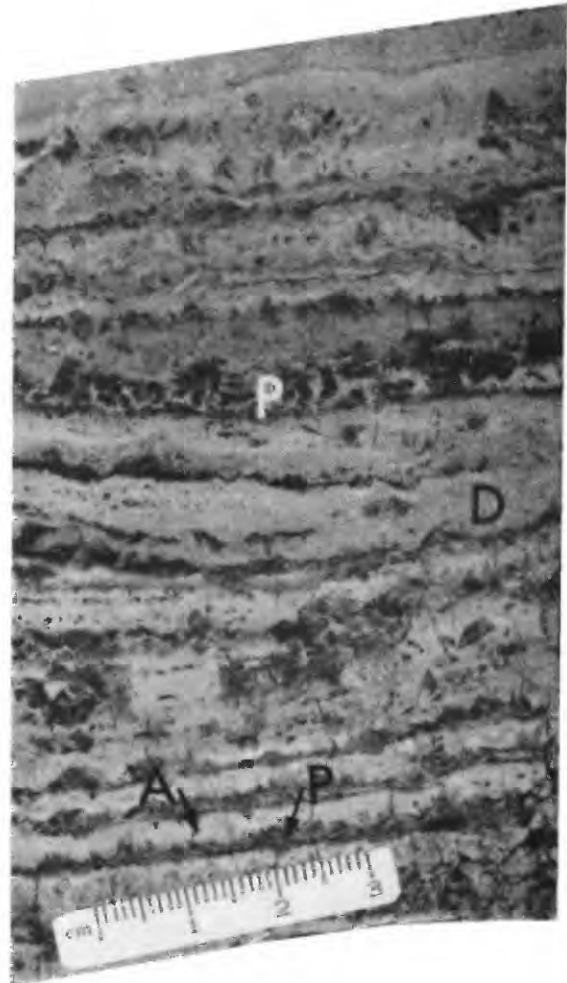


Figure 20. Photograph of polished surface of core from Shafer No. 1 core, depth 2,517.5 ft (767.3 m), illustrating an interval of interbedded dolomite (D) and anhydrite (A) that contains small pseudomorphs (P) after bottom-growth gypsum in regressive phase in upper part of interbeds in cycle 3. Location of core shown in figure 5.

of basin filling. This depositional sequence fits the model for deep-water evaporites described by Schmalz (1969).

The upper part of the regressive anhydrite unit contains a zone of coarse pseudomorphs of anhydrite and halite after gypsum (fig. 5). This pseudomorphic texture in cycle 3 is illustrated from both cores in figures 23–25. In the Cane Creek core this zone is 8.2 ft (2.5 m) thick. The top of this zone of pseudomorphs is conformably overlain by bedded halite.

The pseudomorphic zone, which is common to all cycles in the upper part of the Paradox Formation, must somehow be related to conditions of rising salinity in the basin because the anhydrite lithology grades upward into the overlying halite bed. Whatever the conditions were that fostered development of large gypsum crystals at the top of the interbeds, these conditions were repeated during each cycle.

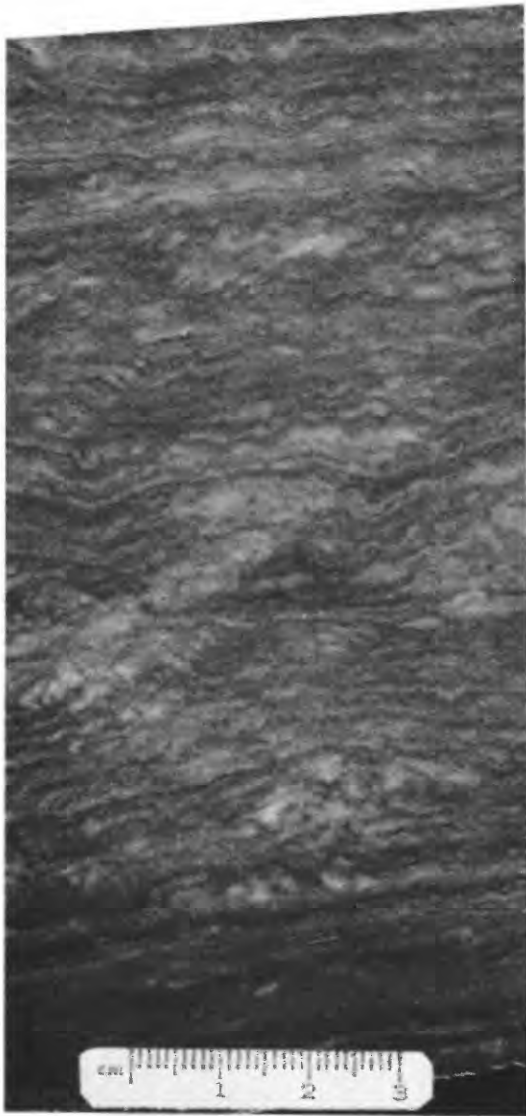


Figure 21. Photograph of polished surface of core from Cane Creek No. 1 core, depth 2,366 ft (721.2 m), illustrating fine, wavy laminations in regressive anhydrite in upper part of interbeds in cycle 3. Location of core shown in figure 5.

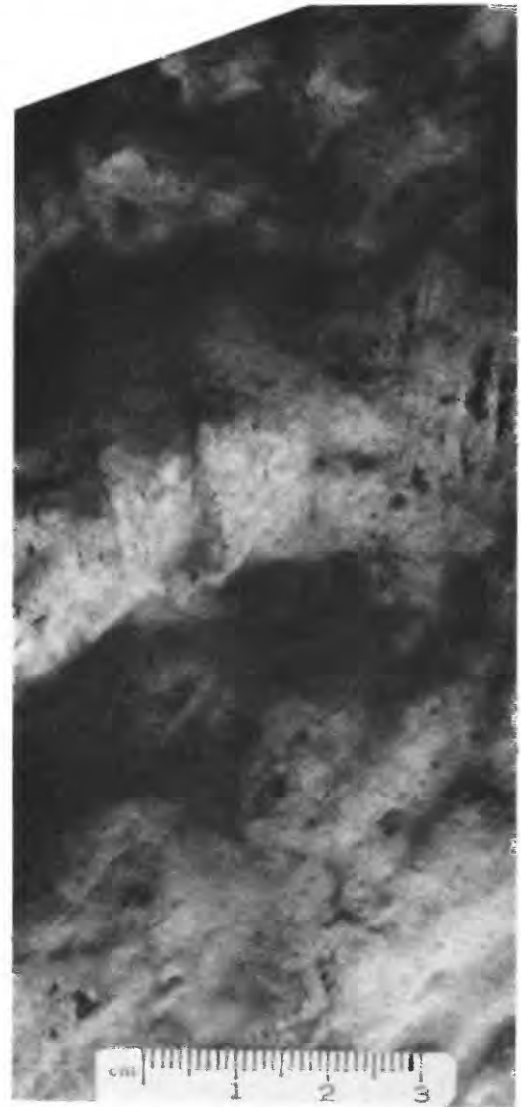


Figure 22. Photograph of polished surface of core from Cane Creek No. 1 core, depth 2,364.2 ft (720.6 m), illustrating a zone of faint pseudomorphic structures and patches of extremely finely laminated anhydrite that may be pseudomorphs after stromatolitic limestone in upper part of interbeds in cycle 3. Location of core shown in figure 5.

Each of the interbeds in all of the cycles observed in the Cane Creek and Shafer cores exhibits the same kinds of contacts as those in cycles 2 and 3. In each there is a sharp contact between the anhydrite at the base of the interbeds and the underlying halite beds, and each of the interbeds has an anhydrite interval at the top that grades into the overlying halite bed through a zone of pseudomorphs. Not all of the interbeds contain black shale, but all contain dolomite and anhydrite.

HALITE BEDS

The halite bed of cycle 3 in the Cane Creek core is 134 ft (40.8 m) thick and is in gradational contact with the inter-

beds of cycle 3 below and in sharp contact with the overlying interbeds of cycle 2 (fig. 2). The halite crystals are clear to slightly cloudy; some are smoky gray to light tan. The cloudiness is due to minute inclusions of brine or very small crystals of anhydrite. The tan coloration is due in some halite to inclusions of organic matter and in some halite to inclusions of fluid hydrocarbons. The halite crystals normally range in size from 2 to 5 mm. The halite bed contains thin laminae of anhydrite that are spaced about 6 in. (15 cm) apart near the top of the halite bed. Downward the anhydrite laminae are closer spaced, and spacing near the base is about 1–2 in. (2.5–5.0 cm). For the most part the anhydrite is in distinct, dense laminae (figs. 26–28). Some laminae, however, have a distinctive texture that we have called “snow-on-the-roof.”

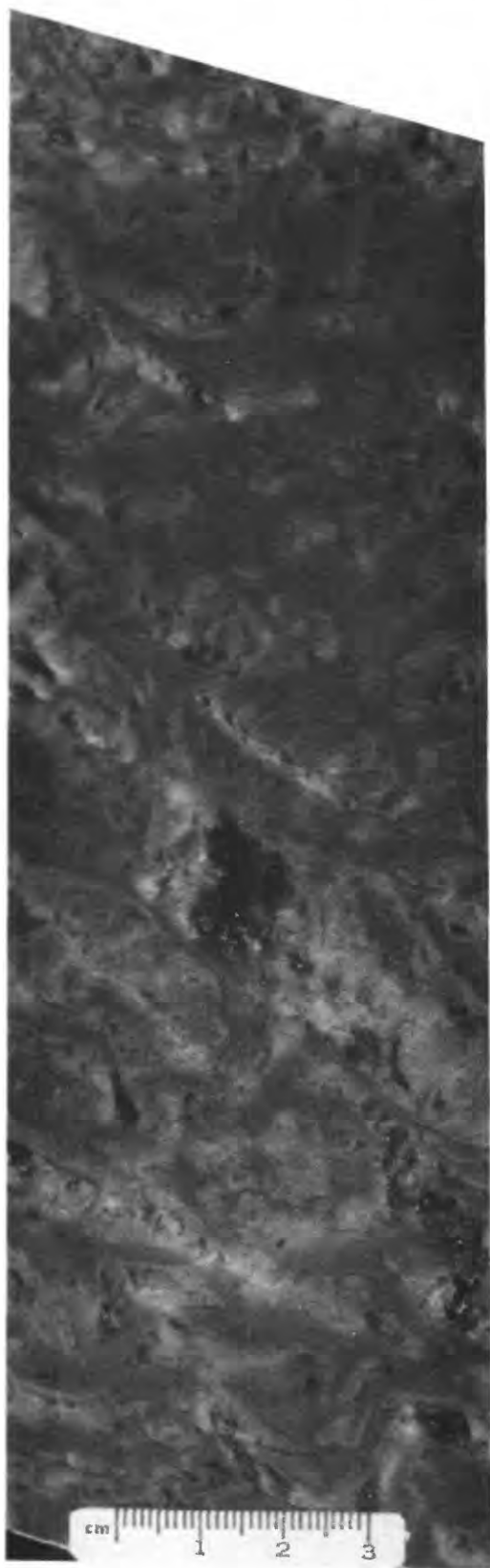


Figure 23. Photograph of polished surface of core from Cane Creek No. 1 core, depth 2,356.7 ft (718.3 m), illustrating coarse pseudomorphic texture of anhydrite and halite after gypsum at top interbeds in cycle 3. Location of core shown in figure 5.

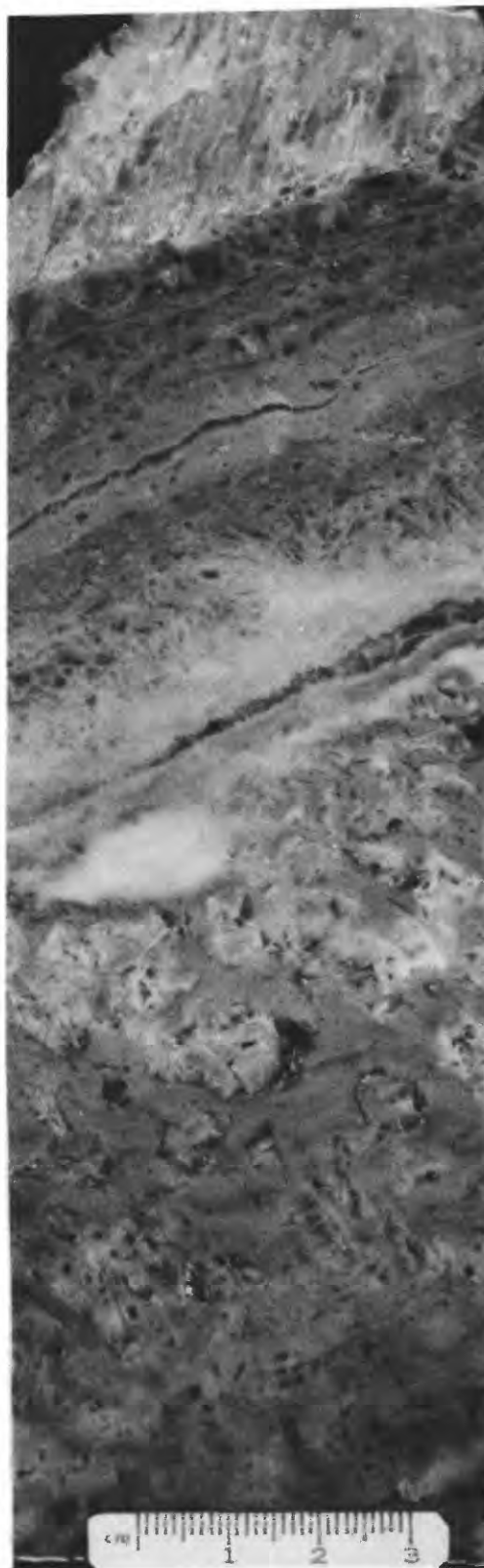


Figure 24. Photograph of polished surface of core from Cane Creek No. 1 core, depth 2,353.7 ft (717.4 m), illustrating coarse pseudomorphic texture of anhydrite and halite after gypsum at top of interbeds in cycle 3. Location of core shown in figure 5.



Figure 25 (above and facing page). Photographs of polished surfaces of core from Shafer No. 1 core at consecutive depths illustrating coarse pseudomorphic texture of anhydrite and halite after gypsum at top of interbeds in cycle 3. Some especially good examples of swallow-tail morphology of the pseudomorphs are shown in *B*. Location of core shown in figure 5. *A*, 2,500 ft (762.0 m). *B*, 2,502 ft (762.6 m). *C*, 2,505 ft (763.5 m).

Examples of this texture are illustrated in figures 29–32. The origin of the anhydrite laminae and the snow-on-the-roof texture is discussed later.

Two of the anhydrite laminae near the base of the halite bed of cycle 3 contain an array of crystals that are pseudomorphs of halite and anhydrite after gypsum (figs. 33, 34). The two layers in the Shafer core are within 3 ft (1 m) of each other (fig. 5), and the lower of the two is illustrated in figure

33. The two pseudomorphous layers in the Cane Creek core are separated more widely than those in the Shafer core (fig. 5). The upper layer is illustrated in figure 34. These two pseudomorphous layers, near the base of the halite bed in each core, are probably correlative. The top of the halite bed of cycle 3 is truncated by the disconformity that separates this halite bed from the interbeds of the overlying cycle 2 (fig. 35).



ANHYDRITE LAMINATIONS

The halite beds of the Paradox Basin contain laminations of anhydrite in intervals that are more widely spaced at the top than at the base. These laminations are 0.03–0.09 in. (0.5–2 mm) thick, and the intervening halite layers are 0.75–6.0 in. (2–15 cm) thick. Typical anhydrite-halite couplets were described by Holser (1979, p. 283) as alternations of clear to translucent halite and dark to black halite. The dark color is caused by a dispersion of anhydrite crystals that diffuse the light. In the halite rocks of the Paradox Basin, the darker layers contain a discrete layer of gray anhydrite. Excellent examples of anhydrite laminations in

halite rocks of the Paradox Basin are illustrated in figures 26–28.

The rhythmic occurrence of anhydrite laminations in halite rocks has been described in rocks attributed to be of marine origin from many deposits of many ages from around the world (Lotze, 1957; Borchert and Muir, 1964; Borchert, 1969; Braitsch, 1971). Anhydrite laminations in halite, other than those in the Paradox Basin, are found in the Permian Castile and Salado Formations of Texas and New Mexico (Dean and Anderson, 1978; Holser, 1979); the Permian Zechstein of Germany (Richter-Bernburg, 1955; Lotze, 1957; Borchert, 1969); the Upper Permian Zechstein of Poland (Czapowski and others, 1990); the Permian Upper Kama deposits of the former U.S.S.R. (Fiveg, 1948; Vakhramayeva, 1956); the Devonian Prairie Evaporite in Saskatchewan, Canada (Wardlaw and Schwerdtner, 1966); and Upper Silurian evaporites of the Michigan Basin (Dellwig, 1955; Dellwig and Evans, 1969; Kunasz, 1970).

Evidence for the origin of anhydrite laminations in the halite rocks of the Paradox Basin may be provided by the occasional anhydrite layers that have a texture that we have called snow-on-the-roof. This texture, described by Hite (1985, p. 225), is composed of the draping of a layer of anhydrite on the uneven top surface of coarse (as much as 0.39 in. (1 cm)), angular, bottom-growth crystals of halite (figs. 29–32) and gives the impression of snow that has fallen on angular roof tops. The occurrence of anhydrite only on the tops of these crystals is interpreted to mean that the halite bottom-growth crystals were in place at the time of calcium sulfate deposition and that the calcium sulfate rained down from the overlying column of brine. There is no evidence to indicate whether the anhydrite was primary or whether the original precipitate was gypsum. In any event, the present anhydrite is very fine grained, and there is no evidence of preexisting gypsum. We conclude that the snow-on-the-roof texture indicates that both the halite and associated anhydrite were the result of subaqueous crystallization.

Stewart (1963, p. 5) suggested that the periodicity of the anhydrite laminations could be explained by periodic (probably annual) climatic temperature changes that would have controlled the temperature of the brine body, or at least the upper layers of the brine body. The solubility of calcium sulfate is dependent on temperature, calcium sulfate being more soluble in cold solutions than in warm. Cyclic temperature fluctuations, therefore, could have precipitated calcium sulfate (probably gypsum) during the summer months and not during the winter months. Periodic, rapid precipitation would have caused a rain of gypsum (anhydrite) crystals onto bottom-growth crystals of halite. An example of this mechanism for the formation of anhydrite laminations in halite in the Permian Zechstein of Poland was described by Czapowski and others (1990).

Anhydrite laminations could also have resulted from periodic influx of meteoric waters that carried calcium bicarbonate into the basin (Hite, 1985; Magaritz, 1987). The

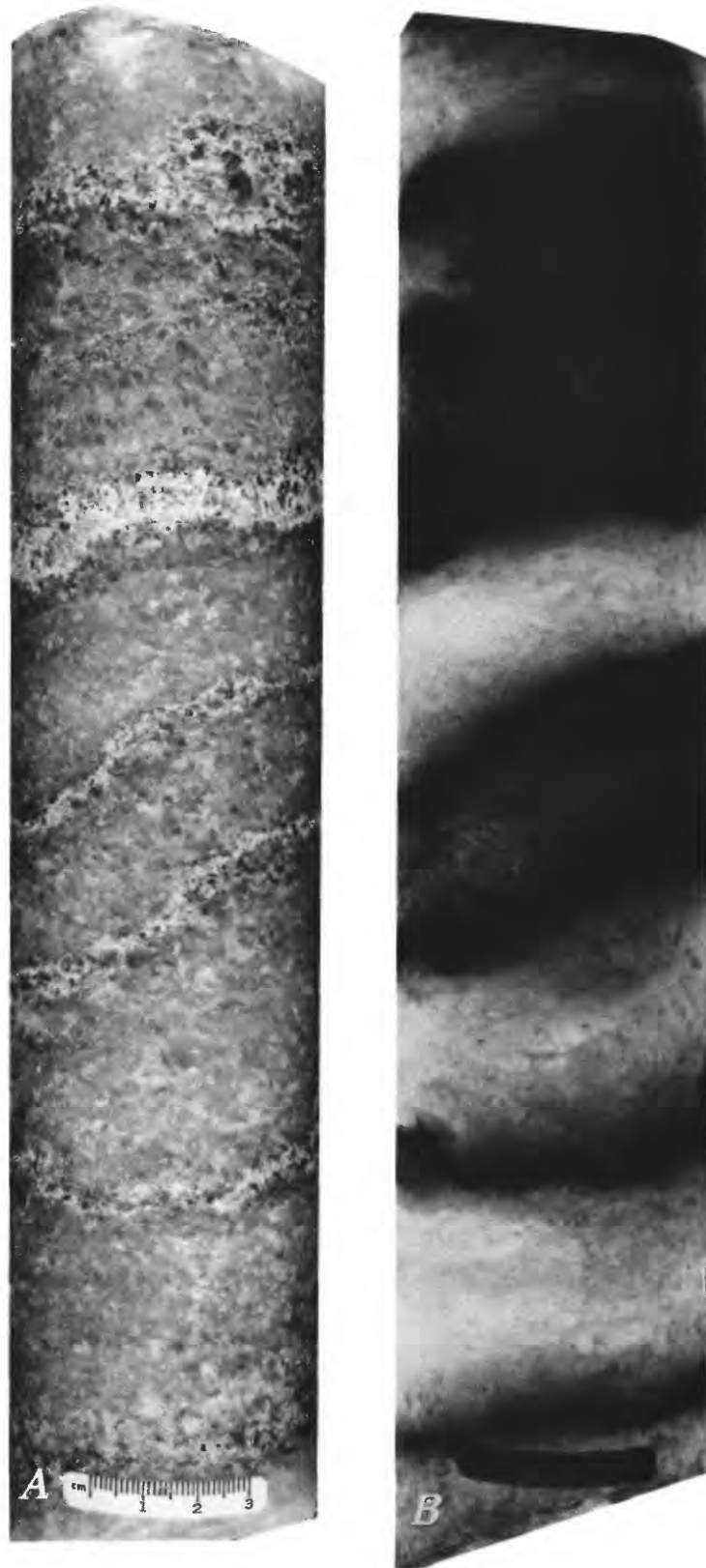


Figure 26. Photographs of segment of Cane Creek No. 1 core, depth 2,336.5 ft (712.2 m). Location of core shown in figure 2. *A*, Reflected light. Anhydrite laminae appear as light-colored layers within the gray halite of the halite bed in cycle 3. *B*, Transmitted light. Optical density results from significant amount of anhydrite disseminated in halite between discrete laminae.

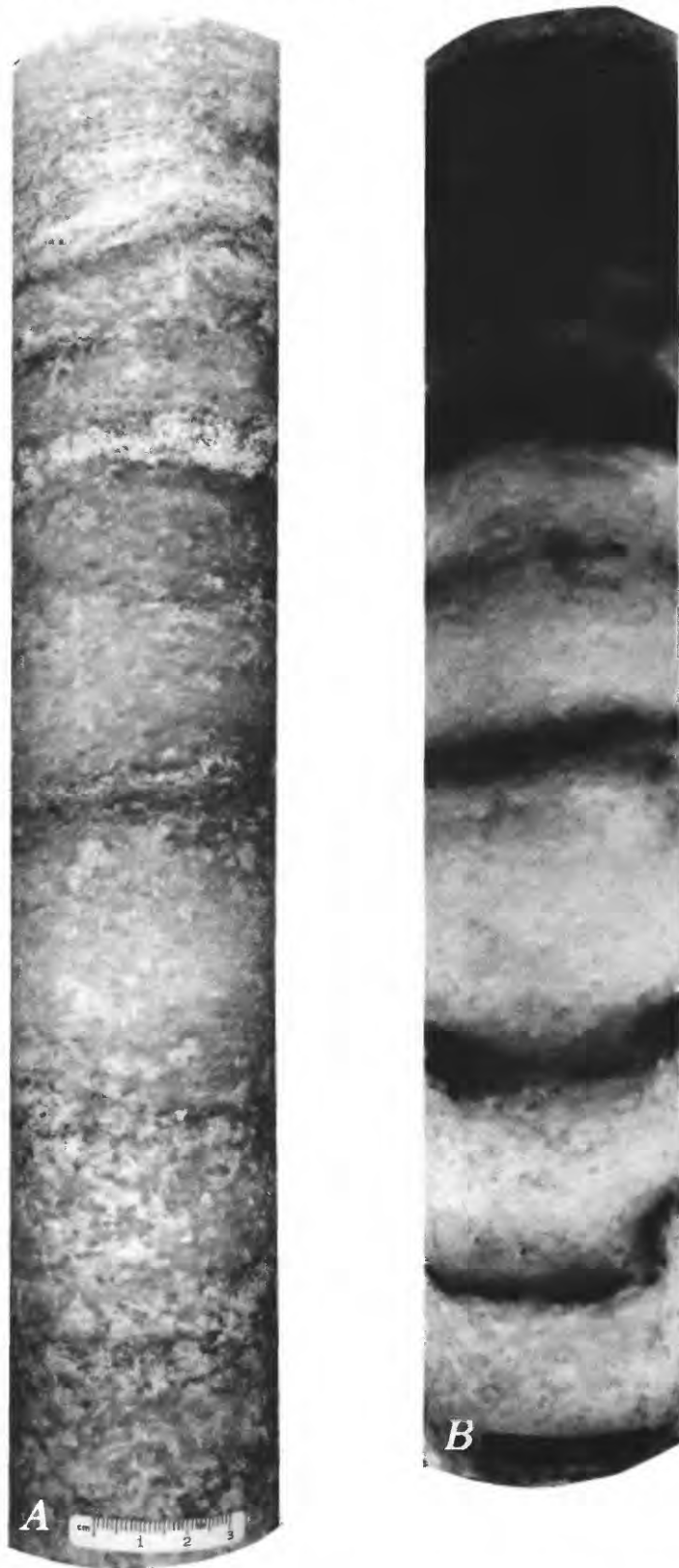


Figure 27. Photographs of segment of Cane Creek No. 1 core, depth 2,265 ft (690.4 m). Location of core shown in figure 2. *A*, Reflected light. Anhydrite laminae appear as light-colored layers within the gray halite of the halite bed in cycle 3. *B*, Transmitted light. Similar to figure 26*B*, the large dark area near the top of the core shows the optical density caused by significant amounts of anhydrite disseminated in the halite between the discrete laminae.

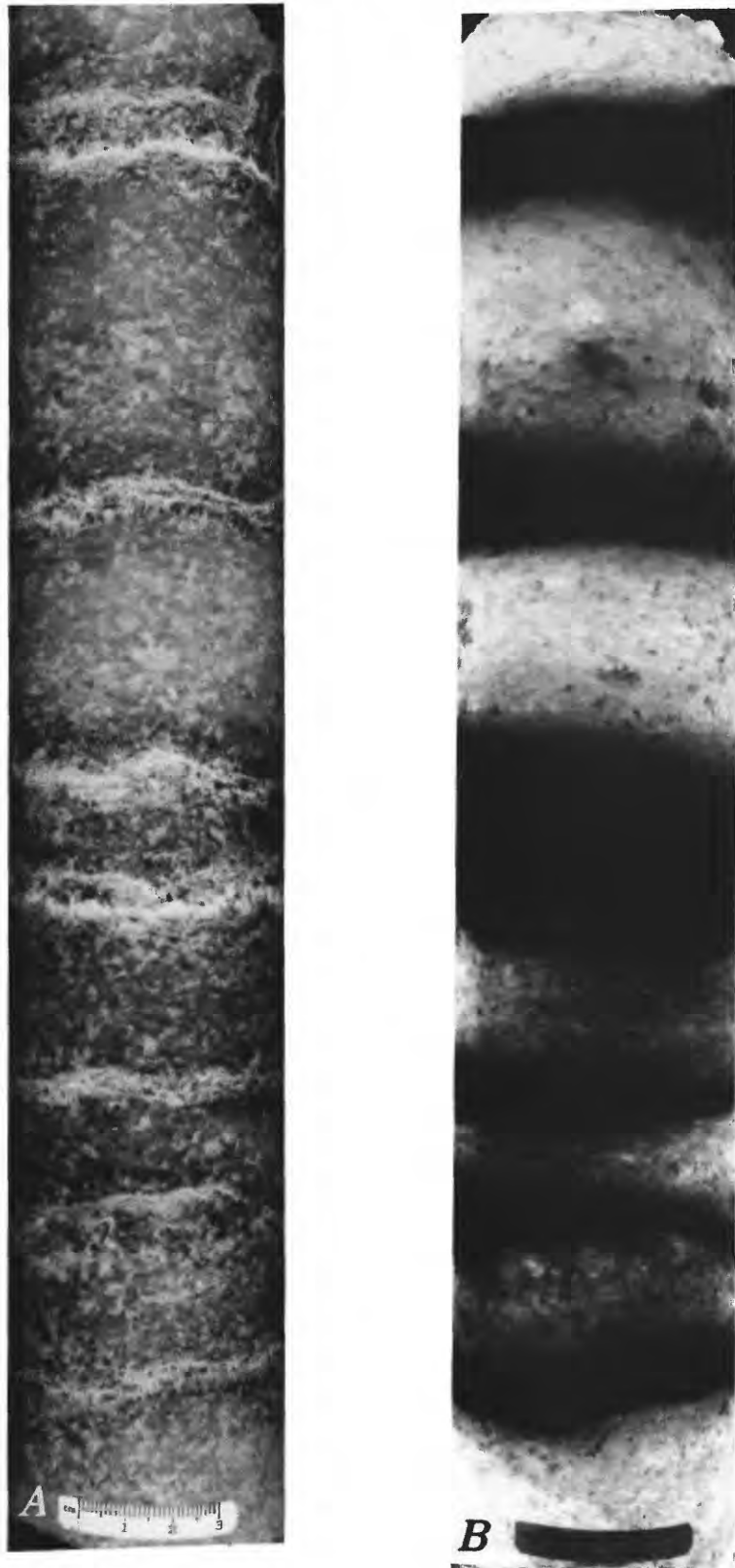


Figure 28. Photographs of segment of Shafer No. 1 core, depth 2,860 ft (871.7 m), illustrating an unusually clear example of halite-anhydrite couplets in halite bed 5. Location of core shown in figure 3. *A*, Reflected light. *B*, Transmitted light.

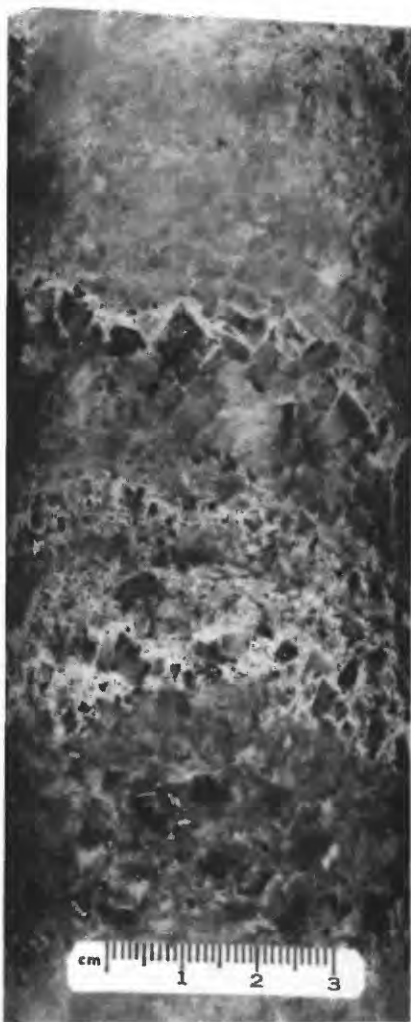


Figure 29. Photograph of segment of Shafer No. 1 core, depth 3,673 ft (1,119.5 m), illustrating snow-on-the-roof texture in halite bed of cycle 9. Location of core shown in figure 3.

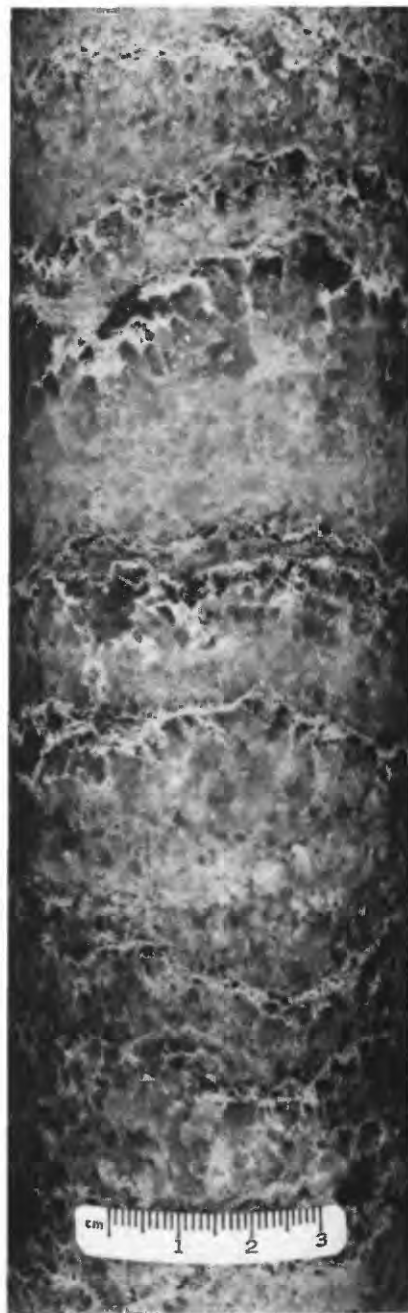


Figure 30. Photograph of segment of Cane Creek No. 1 core, depth 2,623.5 ft (799.6 m), illustrating snow-on-the-roof texture in halite bed of cycle 4. Location of core shown in figure 2.

calcium would react with sulfate in the basin brines to precipitate gypsum or anhydrite. If such influxes were the result of seasonal (annual) storm cycles, then the resultant periodic precipitation of calcium sulfate would have had the same effect as annual temperature fluctuations.

In the Paradox Formation, the thickness of the halite part of the halite/anhydrite couplets generally increases from the bottom to the top of the halite beds. This is especially obvious in the halite beds of cycles 2–5 in the Cane Creek core and in the halite beds of cycles 4–8, 10, and 11 in the Shafer core (Raup and Hite, 1991a, b). In addition to the upward thickening of the halite part of the couplets, the halite layers in the upper parts of the halite beds contain less disseminated anhydrite and organic matter.

The upward thickening of the halite in the couplets would indicate an increased rate of halite precipitation

throughout the deposition of the halite bed if the anhydrite laminations were deposited annually or at some other regular interval. Halite would have been deposited relatively faster through time if the brines in the basin were becoming more concentrated in the more soluble constituents in the sea water, such as the potassium and magnesium chlorides, through a salting-out mechanism that was operating along



Figure 31. Photograph of segment of Cane Creek No. 1 core, depth 2,616.5 ft (797.5 m), illustrating snow-on-the-roof texture in halite bed of cycle 4. Location of core shown in figure 2.

with normal evaporative concentration (Raup, 1970; Braitsch, 1971). The precipitated halite would also be cleaner upward in the halite bed because coprecipitated anhydrite and organic constituents in the brine would have been diluted by the increased halite precipitation.



Figure 32. Photograph of segment of Shafer No. 1 core, depth 2,610.5 ft (795.7 m), illustrating snow-on-the-roof texture in halite bed of cycle 4. Location of core shown in figure 3.

BROMINE DISTRIBUTION

Bromine accumulates in sea-water brines when the brines are concentrated through evaporation. Because a constant, small part of this bromine is incorporated in halite (substituting for chlorine) as it is precipitated, the bromine content in halite reflects the amount of bromine in the brine and serves as an index of the concentration (salinity) of the brine (Raup, 1966; Raup and Hite, 1978). Bromine distribution profiles for the halite beds of cycles 2 and 3 (figs. 36, 37) are very regular; bromine generally increases



Figure 33. Photograph of segment of Shafer No. 1 core, depth 2,491 ft (759.3 m), illustrating layer of pseudomorphic crystals of anhydrite and halite after gypsum on top of thin lamina of anhydrite. This layer is one of only two such layers in lower part of halite bed in cycle 3. Location of core shown in figures 3 and 5.

from bottom to top, typical of the thick halite beds of the Paradox Basin evaporites (Raup, 1966; Raup and Hite, 1978; Hite, 1983) and in general accordance with theoretical considerations (Holser, 1966, 1979; Borchert, 1969).

There are three dominant trends in the profile of the bromine content for the halite bed of cycle 2. Starting at the bottom of the halite bed bromine content is 180 ppm, it decreases upward to 70 ppm, then increases to 160 ppm, and finally decreases in the upper part of the halite bed (Raup, 1966). The last two trends probably correspond to changes in basin salinity during the deposition of this halite bed. The initially high and then decreasing bromine content in the basal 24 ft of halite could also reflect changes in basin salinity; however, it is more likely that this high bromine content



Figure 34. Photograph of segment of Cane Creek No. 1 core, depth 2,340.4 ft (713.3 m), illustrating layer of pseudomorphic crystals of anhydrite and halite after gypsum on top of thin lamina of anhydrite. This layer is one of only two such layers in lower part of halite bed in cycle 3. Location of core shown in figures 2 and 5.

at the base is due to expulsion of residual, bromine-rich brines from the underlying sediments during lithification (Raup and Hite, 1978). From 2,088 to 1,950 ft (636.4–594.4 m), the salinity of the brine generally increased, yet the frequent changes in the slope of the profile, which indicate a rhythmic increase and decrease of bromine in the halite, indicate that the increase in salinity of the brine was interrupted four times by brine dilution that probably resulted from influx of sea water into the basin. Subsequently, during deposition of the upper 14 ft (4.3 m) of the halite bed, the salinity of brine decreased rapidly, probably as the result of increased circulation into the basin. Rocks not far above the



Figure 35. Photograph of segment of Cane Creek No. 1 core, depth 2,218.5 ft (676.2 m), illustrating sharp contact (arrow) between top of the halite bed of cycle 3 and overlying laminated anhydrite at base of cycle 2 interbeds. Location of core shown in figure 2.

halite bed of cycle 2 are predominantly normal marine limestone of the Honaker Trail Formation of the Hermosa Group (Raup and Hite, 1991a, b).

The bromine content of the cycle 3 halite bed similarly generally increases from bottom to top. At the base of the halite bed of cycle 3 the bromine content is 90 ppm. The slightly higher bromine content at the base of this halite bed was probably derived from residual, bromine-rich brines that were expelled from the underlying rocks during lithification similar to the halite bed in cycle 2. Above the basal part of the profile, bromine content decreases to 72 ppm at 2,328 ft (709.6 m). From 2,328 to 2,230 ft (709.6–679.7 m), it increases to 130 ppm but with enough irregularities to suggest the existence of minor salinity variations, similar to those in the halite bed of cycle 2. The bromine content of the upper 10 ft (3 m) of the halite bed of cycle 3 very greatly increases, so much so, in fact, that at the top of the bed the salinity is just short of that necessary for the precipitation of potash minerals (Raup, 1966).

The bromine profiles of the halite beds of cycles 2 and 3 are typical of bromine profiles measured in halite beds of several other cycles in the Paradox Formation (Raup, 1966; Raup and others, 1970; Raup and Hite, 1978; Hite, 1983). The generally regular nature of the profiles indicates that the bromine content of the brines from which the halite precipitated changed gradually during deposition of the halite beds; this gradual change would have required a relatively large volume of brine in the basin. These regular profiles are in contrast to irregular, erratic profiles typical of halite beds deposited from shallow, transitory brines and in geologic settings where the salts were susceptible to episodes of frequent recrystallization (Raup and Hite, 1978).

Bromine profiles for halite beds of the Paradox Formation (Raup, 1966; Raup and Hite, 1978; Hite, 1983) indicate essentially continuous, uninterrupted deposition. The rapidity of salt deposition would require sufficient basin depth to accommodate the entire thickness of at least a single halite bed. The thickest halite bed in the upper part of the Paradox Basin evaporites is the halite bed of cycle 6, which is about 330 ft (100 m) thick. Other halite beds, lower in the stratigraphic section, are several hundred feet thick (Hite, 1960). Wardlaw and Schwerdtner (1966) analyzed the deposition rate of the halite in the Prairie Evaporite of Saskatchewan and concluded that, if the annual sedimentation rate was 5 cm per year, then the 600-ft-thick chloride section in the center of the basin would have formed in less than 4,000 years. Because this sedimentation rate far exceeds any known tectonic subsidence rate, it is assumed that the basin would have been at least that deep prior to halite deposition. Borchert (1969) followed a similar line of reasoning for the depositional rates and tectonic setting of evaporites in the Permian Zechstein Basin of Germany. Following the same reasoning for evaporites of the Paradox Basin, which had an original deposition thickness in excess of 5,000 ft (1,500 m), the lower part of the evaporites must have been deposited in fairly deep water. As the evaporites accumulated, the depth of the water in the basin would have decreased (Schmalz, 1969).

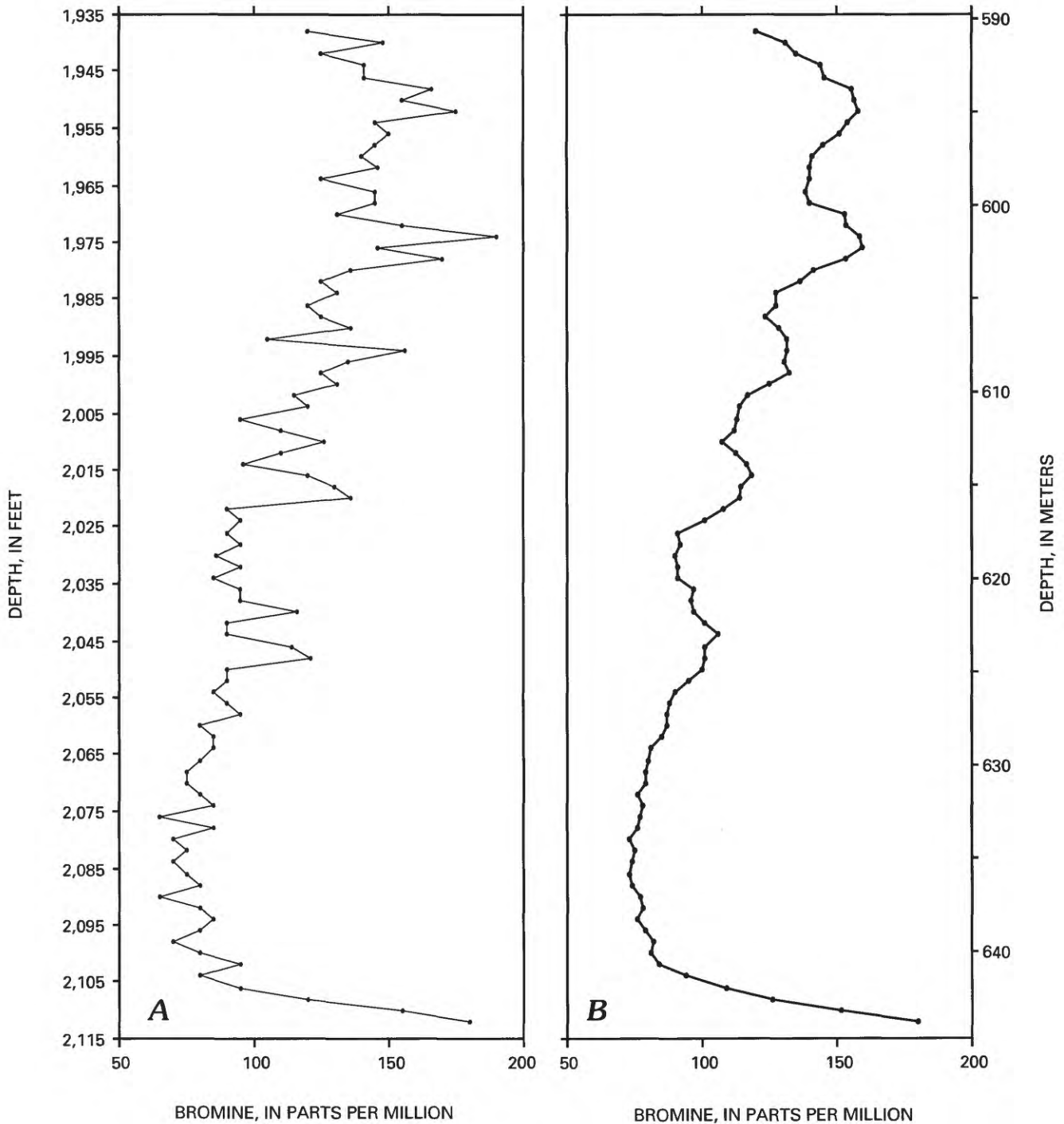


Figure 36. Bromine distribution in halite bed of cycle 2, Cane Creek No. 1 core. *A*, Analytical results. *B*, Smoothed profile using a moving average of five points.

POTASH DEPOSITS

Potash, generally in the form of sylvinite, is in 17 of the 29 evaporite cycles in the Paradox Basin (Hite, 1960). Concentration of the potash at or near the tops of the halite beds, for the most part, indicates the salinity asymmetry of the evaporite cycles. Bromine distribution studies of the halite beds of the Paradox Basin (Raup, 1966; Hite, 1983) show

that salinity of the basin brines increased during deposition of most of the halite beds. The salinity curve for cycle 2 (fig. 4) shows an increase of salinity from the middle of the black shale upward through the interbeds and through the halite bed, in the part of the curve Y through Z. This interval is in the regressive phase of the cycle when the sea level dropped to its low stand, circulation of sea water into the basin was restricted, and salinities within the basin were steadily

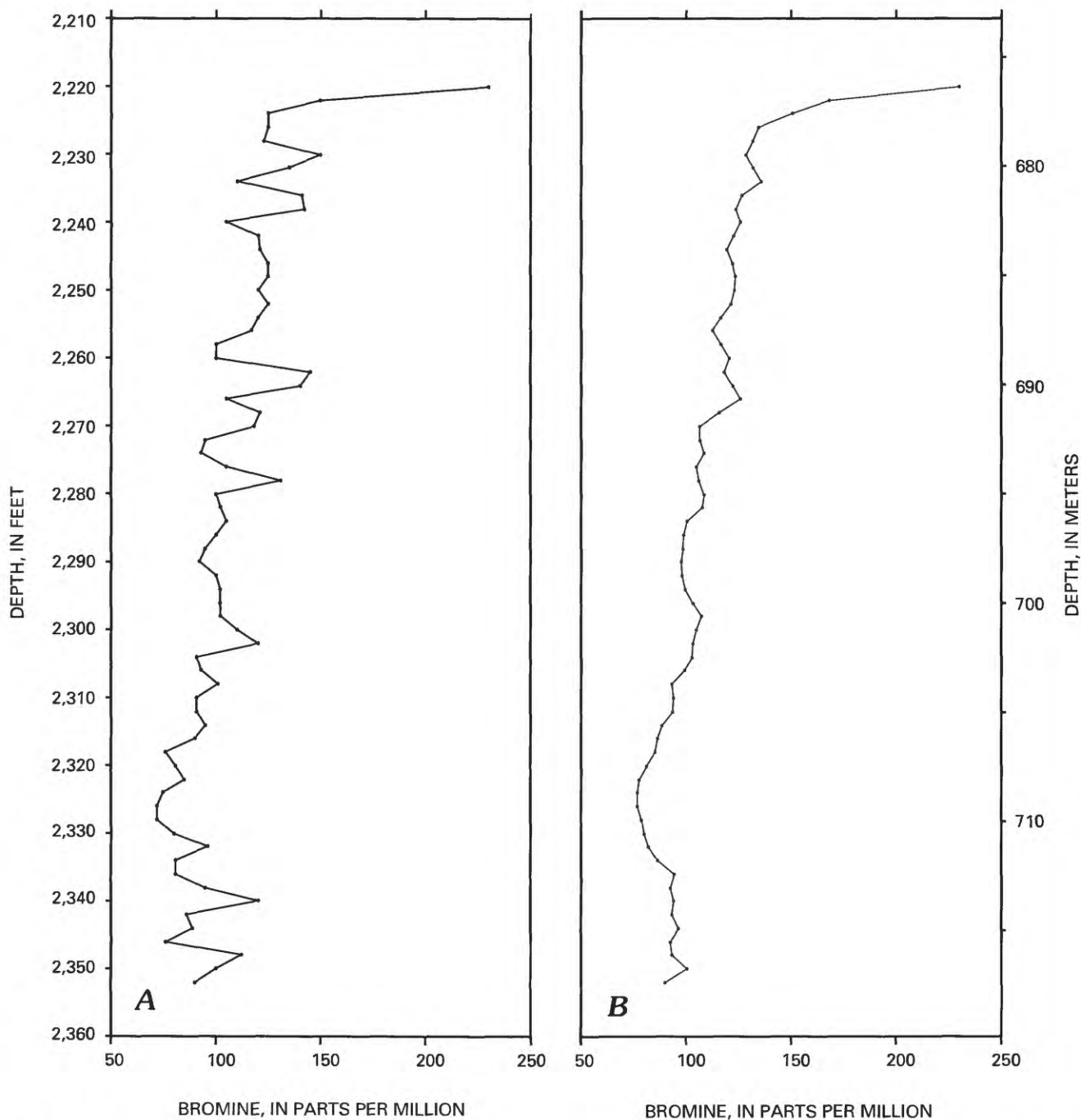


Figure 37. Bromine distribution in halite bed of cycle 3, Cane Creek No. 1 core. *A*, Analytical results. *B*, Smoothed profile using a moving average of five points.

increasing. Potash mineralization is indicative of extreme brine salinities that resulted from extreme aridity during the final stages of those particular cycles.

INTERBED CONTACT RELATIONSHIPS

All of the interbeds in each of the cycles observed in the Cane Creek and Shafer cores are identical with respect to

their upper and lower contacts. These contact relationships are well illustrated in cycle 3 (fig. 5). In cycle 3 the base of the interbeds is in sharp contact with the underlying halite bed of cycle 4 (figs. 7, 8), and the upper contact is gradational with the halite bed of cycle 3 through a zone of coarse pseudomorphs of anhydrite and halite after gypsum (figs. 23–25). Photographs of these contact relationships in cycles other than 3 are illustrated in figures 38–45.

The sharp, disconformable basal contacts of interbeds in cycles 2, 4, 6, 8, and 10 are illustrated in figures 38–41.



Figure 38. Photograph of polished surface of core from Shafer No. 1 core, depth 2,655 ft (809.2 m), illustrating sharp contact (arrow) between finely laminated anhydrite at base of interbeds at base of cycle 4 and underlying halite bed at top of cycle 5. Location of core shown in figure 3.

The locations of the photographic figures in the Cane Creek core are indicated by arrows in figure 2, those in the Shafer core in figure 3.

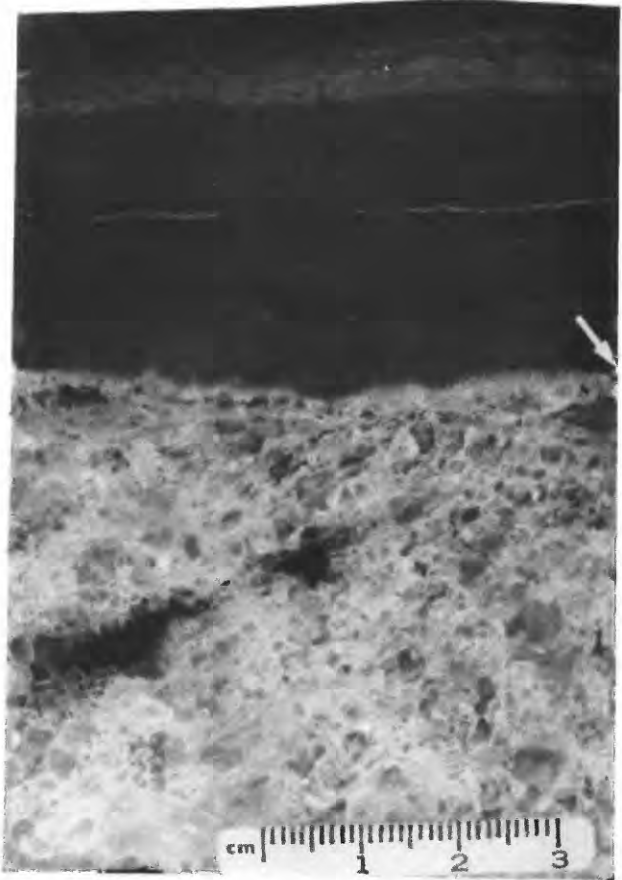


Figure 39. Photograph of polished surface of core from Shafer No. 1 core, depth 3,303 ft (1,006.7 m), illustrating sharp contact (arrow) between finely laminated anhydrite at base of interbeds at base of cycle 6 and underlying halite bed at top of cycle 7. Black areas within the halite are organic matter. Location of core shown in figure 3.

The gradational pseudomorphic zones of the upper contacts of interbeds in cycles 4, 5, 11, and 13 are illustrated in figures 42–45. In these upper contact zones, which are 1–3 ft (0.30–1 m) thick, anhydrite grades upward to halite with no sharply defined contact.

DETAILED CORRELATION OF CYCLE 3 INTERBEDS BETWEEN CANE CREEK NO. 1 AND SHAFER NO. 1 CORE HOLES

The degree to which correlations of lithologic units can be made between core holes is indicative of uniformity of deposition in a sedimentary basin. The lithology and texture of interbeds at the base of cycle 3 in both the Cane Creek and Shafer core holes are sufficiently distinct to make detailed correlation possible (fig. 5). These two core holes are about 5 mi (8 km) apart. Although this is not a great distance in a

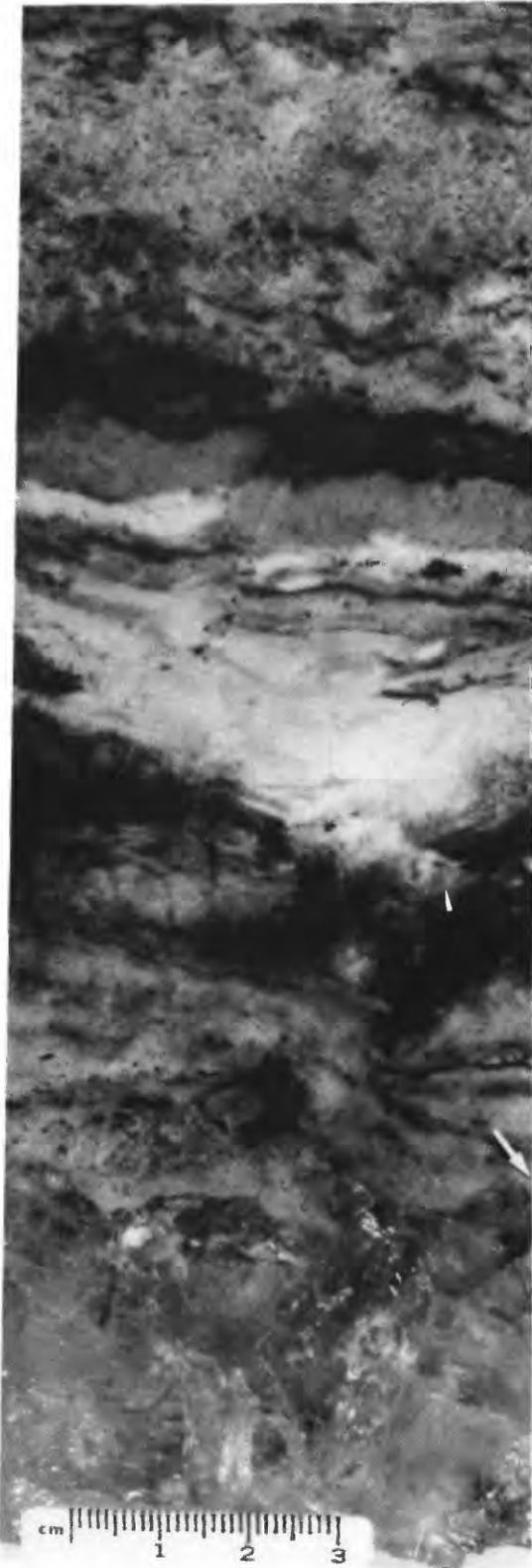


Figure 40. Photograph of polished surface of core from Shafer No. 1 core, depth 3,528.5 ft (1,075.5 m), illustrating sharp contact (arrow) between layered anhydrite at base of interbeds at base of cycle 8 and underlying glassy halite in halite bed at top of cycle 9. Location of core shown in figure 3.



Figure 41. Photograph of segment of Shafer No. 1 core, depth 3,892 ft (1,186.3 m), illustrating sharp contact (arrow) between layered anhydrite at base of interbeds at base of cycle 10 and underlying halite bed at top of cycle 11. Location of core shown in figure 3.

basin the size of the Paradox Basin, it is sufficient distance to require conditions of uniform deposition in this part of the basin through the time required for the accumulation of these interbeds. Thus, correlation of thin units over this distance indicates water that was deep enough that the bottom was not disturbed by waves and currents. Dense bottom brines would have also inhibited activity of burrowing organisms.

The base of the interbeds in both the Cane Creek and Shafer core holes is composed of finely laminated anhydrite (figs. 7 and 9 in the Cane Creek core and fig. 8 in the Shafer core). The laminated anhydrite grades upward into nodular anhydrite (figs. 9 and 10 in the Cane Creek core and figs. 11 and 12 in the Shafer core). The nodular interval is thicker in the Cane Creek core than in the Shafer core. The overlying silty dolomite is about the same thickness in both holes. A very distinct thin black shale interval near the middle of the dolomite is somewhat thicker in the Cane Creek core than in the Shafer core. There are, however, no distinct correlatable units in the black shale. The silty dolomite above the black shale is about the same thickness in both core holes, but here too, there are no correlatable units.

The upper anhydrite has several distinctive lithologic units. The lowest unit in this regressive anhydrite is laminated but has small pseudomorphs after gypsum. This unit in the Cane Creek core is illustrated in figure 19 and in the Shafer core in figure 20. In both cores this unit is overlain by a thin interval that has thin, parallel laminations (fig. 21). Above the thin parallel laminations is a zone of very thin laminations that may be replacements of algal (stromatolitic) limestone (fig. 22). Overlying this unit is the zone of coarse pseudomorphs after gypsum that grades upward into the overlying halite bed. The coarse pseudomorphs are illustrated in figures 23 and 24 for the Cane Creek core and in figure 25 for the Shafer core.

Because of the similarity between interbeds of cycle 3 and interbeds of the other cycles, it is not unreasonable to assume that conditions were similar during deposition of all of the cycles of the upper part of the Paradox Formation.

SEA-LEVEL CONTROL DURING EVAPORITE DEPOSITION

Peterson and Ohlen (1963) and Hite and Buckner (1981) attributed the cyclicity of the Paradox Basin evaporites to periodic changes in sea level in response to advance and retreat of glaciers in Gondwanaland during Pennsylvanian time. Interglacial melting would cause a rise in sea level that would increase water depths in the shelf



Figure 42 (facing column). Photograph of segment of Cane Creek No. 1 core, depth 2,640.5 ft (804.8 m), illustrating coarse pseudomorphous texture of anhydrite and halite after gypsum at top of interbeds in cycle 4. Location of core shown in figure 2.

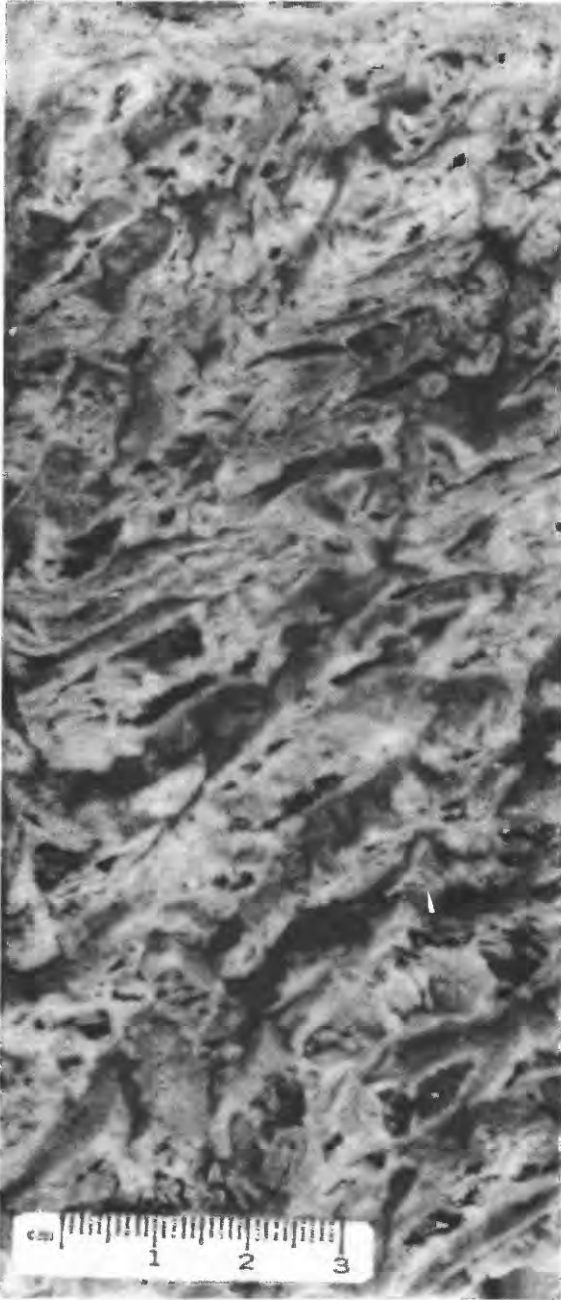


Figure 43. Photograph of polished surface of core from Shafer No. 1 core, depth 2,869.5 ft (874.6 m), illustrating coarse pseudomorphic texture of anhydrite and halite after gypsum at top of interbeds in cycle 5. Location of core shown in figure 3.

areas of the Paradox Basin resulting in an increase in circulation and a lowering of salinity of the basin waters. This freshening of the basin brines would cause dissolution of the upper layers of previously deposited halite and produce a disconformity onto which the overlying anhydrite of succeeding cycles was deposited. The buildup of Gondwanaland glaciers would have caused a lowering of sea level that

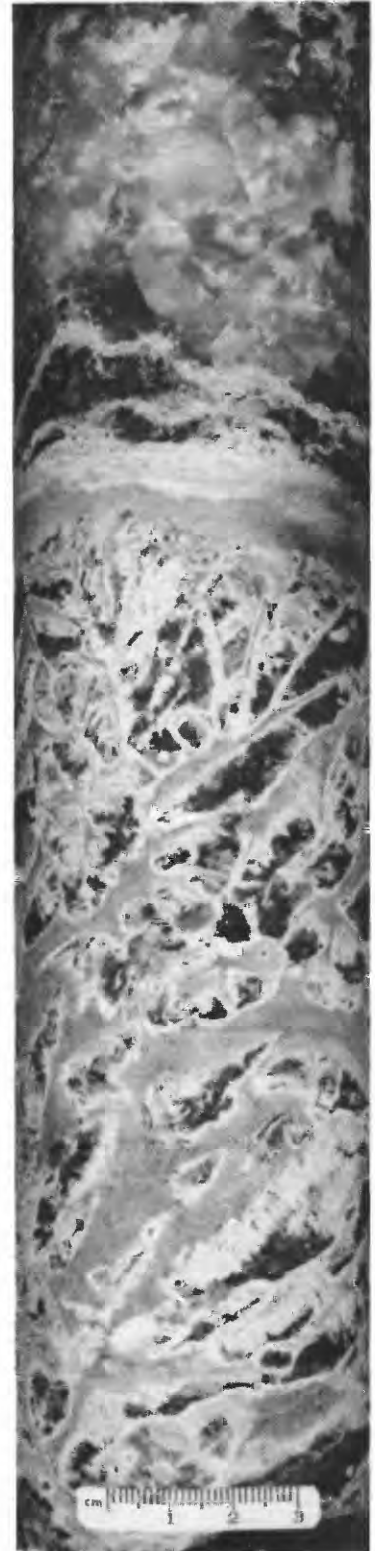


Figure 44. Photograph of polished surface of core from Shafer No. 1 core, depth 3,919.5 ft (1,194.7 m), illustrating coarse pseudomorphic texture of anhydrite and halite after gypsum at top of interbeds in cycle 11. Location of core shown in figure 3.



Figure 45. Photograph of polished surface of core from Shafer No. 1 core, depth 4,149.5 ft (1,264.8 m), illustrating coarse pseudo-morphic texture of anhydrite and halite after gypsum at top of interbeds in cycle 13. Location of core shown in figure 3.

would restrict circulation in the Paradox Basin, causing a rise in salinity of the basin brines and the deposition of a sequence of precipitates of increasing salinity. It is possible that the evaporite cycles of the Paradox Basin, which probably formed in response to the Gondwanaland glacial cycles, could be correlated with the numerous Pennsylvanian cyclotherms of the Midcontinent region of the United States.

SUMMARY OF EVIDENCE FOR ENVIRONMENTS OF DEPOSITION OF EVAPORITES IN THE PARADOX BASIN

In the foregoing discussion several lines of evidence indicate (1) that evaporites of the Paradox Basin were deposited in a silled basin in which the sill was a broad, shallow shelf along the northwest, west, south, and southeast sides of the basin and (2) that the northeast side of the basin was bounded by the Uncompahgre Uplift, which was probably a prominent range of mountains during Desmoinesian time. The basin had probably become quite deep prior the deposition of the first evaporites. Further work is needed to determine the rates of tectonic subsidence of the basin, the depth of the basin at the time of first evaporite deposition, and the rates of evaporite deposition as compared with the rates of basin subsidence.

The following criteria indicate that the evaporites of the Paradox Basin were deposited subaqueously in a brine-filled basin.

1. Concentric distribution of rock types indicates a normal basin configuration for the Paradox Basin. Rock types having the highest solubility are concentrated in the deepest and most restricted part of the basin, whereas those having the lowest solubility are most widespread (fig. 1) (unpublished data). This lithologic distribution, along with characteristics listed below, indicates a regular distribution of brines of differing salinity within the basin (Hite and Buckner, 1981) that would require a dynamic evaporation and circulation system in a basin containing a large volume of brine.

2. Halite crystals in snow-on-the-roof textures are interpreted to be the result of basin bottom growth; anhydrite (gypsum) precipitated in the overlying brine and then rained down onto the halite. Both aspects of this interpretation require a standing body of brine.

3. The progressive increase in thickness of halite in the halite-anhydrite couplets of many of the halite beds is best explained by a progressive change in the chemistry of the brines in the basin that resulted in an increasing precipitation rate of the halite. For such a mechanism, the basin had to contain a relatively large volume of brine.

4. Progressively cleaner halite from bottom to top of a halite bed probably resulted from the dilution effect of

progressively more rapid precipitation of halite from bottom to top that would have incorporated less anhydrite and organic matter during deposition.

5. Bromine profiles for halite beds of the Paradox Formation (Raup, 1966; Raup and Hite, 1978; Hite, 1983) indicate essentially continuous deposition. Because of the inferred rapid rates of halite precipitation, each of the halite beds, or perhaps a series of halite beds, must have been deposited in a deep basin from a relatively large volume of brine (Borchert and Muir, 1964; Wardlaw and Schwerdtner, 1966).

6. Correlatability of thin stratigraphic units over large distances has been accepted in other areas as good evidence for relatively deep basin deposition. The two core holes presented in this study are 5 mi (8 km) apart, and they have several small units that can be correlated with confidence. Although this distance is not as great as some of the distances over which correlations have been made in the Zechstein Basin of Germany or in the Delaware Basin of Texas and New Mexico, it is, nevertheless, a greater distance than correlations could be expected in shallow-water or sabkha environments.

7. The consistent presence of pseudomorphs of halite and anhydrite after gypsum at the top of *each* of the interbeds indicates the regular cyclic recurrence of some mechanism that would most likely occur in a basin with a large volume of brine.

8. Generally gradational contacts between all rock types within each cycle and unconformities between cycles indicate a recurring sequence of sedimentation that is probably controlled by dynamics within the basin brines.

9. On the negative side, the lack of mudcracks, ripple marks, or other indicators of desiccation in the Paradox evaporites within the basin indicates a lack of shallow-water or subaerial conditions within the basin margins.

REFERENCES CITED

- Baker, P.A., and Kastner, M., 1981, Constraints on the formation of sedimentary dolomite: *Science*, v. 213, 10 July, p. 214–216.
- Borchert, Hermann, 1969, Principles of oceanic salt deposition and metamorphism: *Geological Society of America Bulletin*, v. 80, p. 821–864.
- Borchert, Hermann, and Muir, R.O., 1964, Salt deposits: New York, D. Van Nostrand Company, 338 p.
- Braitsch, O., 1971, Salt deposits—Their origin and composition: New York-Heidelberg-Berlin, Springer-Verlag, 297 p.
- Butler, G.P., 1969, Modern evaporite deposition and geochemistry of coexisting brines, the sabkha, Trucial Coast, Arabian Gulf: *Journal of Sedimentary Petrology*, v. 39, p. 70–89.
- Czapowski, G., Antonowicz, L., and Peryt, T.M., 1990, Facies and palaeogeography of the Zechstein (Upper Permian) Older Halite (Na₂) in Poland: *Polish Academy of Sciences Earth Sciences Bulletin*, v. 38, no. 1–4, p. 45–55.
- Dean, W. E., and Anderson, R. Y., 1978, Salinity cycles—Evidence for subaqueous deposition of Castile Formation and lower part of Salado Formation, Delaware basin, Texas and New Mexico, in Austin, G.S., compiler, *Geology and mineral deposits of Ochoan rocks in Delaware Basin and adjacent areas: New Mexico Bureau of Mines and Mineral Resources Circular 159*, p. 1520.
- 1982, Continuous subaqueous deposition of the Permian Castile evaporites, Delaware basin, Texas and New Mexico, in Handford, C.R., Loucks, R.G., and Davies G.R., eds., *Depositional and diagenetic spectra of evaporites: Society of Economic Paleontologists and Mineralogists Core Workshop, 3rd*, Calgary, Canada, 1982, p. 324–353.
- Dean, W.E., Davies, G.R., and Anderson, R.Y., 1975, Sedimentological significance of nodular and laminated anhydrite: *Geology*, v. 3, no. 7, p. 367–372.
- Dellwig, L.F., 1955, Origin of the Salina salt of Michigan: *Journal of Sedimentary Petrology*, v. 25, no. 2, p. 83–110.
- Dellwig, L.F., and Evans, Robert, 1969, Depositional processes in Salina salt of Michigan, Ohio, and New York: *American Association of Petroleum Geologists Bulletin*, v. 53, no. 4, p. 949–956.
- Fiveg, M.P., 1948, The annual cycle of sedimentation of rock salt from the Upper Kama deposit [trans.]: *Doklady Akademii Nauk SSSR*, v. 61, p. 1087–1090.
- Hardie, L.A., 1987, Dolomitization—A critical view of some current views: *Journal of Sedimentary Petrology*, v. 57, no. 1, p. 166–183.
- Harms, J.C., 1974, Brushy Canyon Formation, Texas—A deep-water density current deposit: *Geological Society of America Bulletin*, v. 85, p. 1763–1784.
- Hite, R.J., 1960, Stratigraphy of the saline facies of the Paradox Member of the Hermosa Formation of southeastern Utah and southwestern Colorado, in *Geology of the Paradox basin fold and fault belt: Four Corners Geological Society Field Conference, 3rd*, p. 86–89.
- 1968, Salt deposits of the Paradox basin, southeast Utah and southwest Colorado, in Mattox, R.B., ed., *Saline deposits: Geological Society of America Special Paper 88*, p. 319–330.
- 1970, Shelf carbonate sedimentation controlled by salinity in the Paradox Basin, southeast Utah, in *Third Symposium on Salt: Northern Ohio Geological Society*, v. 1, p. 48–66.
- 1983, Preliminary mineralogical and geochemical data from the Department of Energy Gibson Dome corehole No. 1, San Juan County, Utah: *U.S. Geological Survey Open-File Report 83-780*, 57 p.
- 1985, The sulfate problem in marine evaporites, in *Sixth Symposium on Salt: The Salt Institute*, v. 1, p. 217–230.
- Hite, R.J., Anders, D.E., and Ging, T.G., 1984, Organic-rich source rocks of Pennsylvanian age in the Paradox basin of Utah and Colorado, in Woodward, J., Meissner, F.F., and Clayton, J.L., eds., *Hydrocarbon source rocks of the greater Rocky Mountain region: Rocky Mountain Association of Geologists*, p. 255–274.
- Hite, R.J., and Buckner, D.H., 1981, Stratigraphic correlations, facies concepts, and cyclicity in Pennsylvanian rocks of the Paradox basin: *Rocky Mountain Association of Geologists Field Conference*, 1981, p. 147–159.
- Holser, W.T., 1966, Bromide geochemistry of salt rocks, in *Second Symposium on Salt: Northern Ohio Geological Society*, v. 1, p. 248–275.
- 1979, Mineralogy of evaporites, in Burns, R.G., ed., *Marine minerals: Mineralogical Society of America Reviews in Mineralogy*, v. 6, p. 211–294.
- Kinsman, D.J.J., 1966, Gypsum and anhydrite of Recent age, Persian Gulf, in *Second Symposium on Salt: Northern Ohio Geological Society*, v. 1, p. 302–326.
- Kluth, C.F., and Coney, P.J., 1981, Plate tectonics of the Ancestral Rocky Mountains: *Geology*, v. 9, p. 10–15.
- Kunasz, I. A., 1970, Significance of laminations in the Upper Silurian evaporite deposit of the Michigan basin, in *Third Symposium on Salt: Northern Ohio Geological Society*, v. 1, p. 67–77.
- Lotze, Franz, 1957, *Steinsalz und Kalisalz*, v. 1: Berlin, Gebürder Bornträger, 465 p.
- Mallory, W.W., 1975, Middle and southern Rocky Mountains, northern Colorado Plateau, and eastern Great basin region, in *Paleotectonic investigations of the Pennsylvanian System in the United States*, part

- I—Introduction and regional analyses of the Pennsylvanian System: U.S. Geological Survey Professional Paper 853, p. 265–278.
- Magaritz, M., 1987, A new explanation for cyclic deposition in marine evaporite basin; meteoric water input: *Chemical Geology*, v. 62, p. 239–250.
- Peterson, J.A., and Hite, R.J., 1969, Pennsylvanian evaporite-carbonate cycles and their relation to petroleum occurrence, southern Rocky Mountains: *American Association Petroleum Geologists*, v. 53, no. 4, p. 884–908.
- Peterson, J.A., and Ohlen, H.R., 1963, Pennsylvanian shelf carbonates, Paradox basin, in *Symposium on Shelf Carbonates of the Paradox Basin: Four Corners Geological Society Field Conference*, 4th, Guidebook, p. 65–79.
- Raup, O.B., 1966, Bromine distribution in some halite rocks of the Paradox Member, Hermosa Formation, in Utah, in *Second Symposium on Salt: Northern Ohio Geological Society*, v. 1, p. 236–247.
- 1970, Brine mixing—An additional mechanism for formation of basin evaporites: *American Association of Petroleum Geologists Bulletin*, v. 54, no. 12, p. 2246–2259.
- 1982, Gypsum precipitation by mixing seawater brines: *American Association of Petroleum Geologists*, v. 66, no. 3, p. 363–367.
- Raup, O.B., and Hite, R.J., 1978, Bromine distribution in marine halite rocks, in Dean, W.E., and Schreiber, B.C., eds., *Marine evaporites: Society of Economic Paleontologists and Mineralogists Short Course*, p. 105–123.
- 1991a, Preliminary lithologic and mineralogical data from the Delhi-Taylor Oil Company, Cane Creek No. 1 corehole, Grand County, Utah: U.S. Geological Survey Open-File Report 91–324, 24 p.
- 1991b, Preliminary stratigraphic and lithologic data from the Delhi-Taylor Oil Company, Shafer No. 1 corehole, San Juan County, Utah: U.S. Geological Survey Open-File Report 91–373, 34 p.
- Raup, O.B., Hite, R.J., and Groves, H.L., Jr., 1970, Bromine distribution and paleosalinities from well cuttings, Paradox basin, Utah and Colorado, in *Third Symposium on Salt: Northern Ohio Geological Society*, v. 1, p. 40–47.
- Richter-Bernburg, Gerhard, 1955, Über salinare Sedimentation: *Deutsche Geologische Gesellschaft Zeitschrift*, v. 105, p. 593–645.
- Ross, C.A., 1979, Late Paleozoic collision of North and South America: *Geology*, v. 7, p. 41–44.
- Schmalz, R.F., 1969, Deep-water evaporite deposition—A genetic model: *American Association of Petroleum Geologists Bulletin*, v. 53, no. 4, p. 798–823.
- Stewart, F.H., 1963, Marine evaporites, in *Fleischer, M., ed., Data of geochemistry (6th ed.)*: U.S. Geological Survey Professional Paper 440–Y, 52 p.
- Vakhrameyeva, V.A., 1956, The stratigraphy and tectonics of the Upper Kama deposits [trans.]: *Trudy Vsesoyuznogo Nauchno-Issledovatel'skogo Instituta Galurgii*, v. 22, p. 277–313.
- Wardlaw, N.C., and Schwerdtner, W.M., 1966, Halite-anhydrite seasonal layers in the Middle Devonian Praire Evaporite Formation, Saskatchewan, Canada: *Geological Society of America Bulletin*, v. 77, p. 331–342.

Published in the Central Region, Denver, Colorado
 Manuscript approved for publication March 6, 1992.

